

Temporal dynamics of biogeochemical processes at the Norman Landfill site

Bhavna Arora,^{1,2} Binayak P. Mohanty,¹ Jennifer T. McGuire,³ and Isabelle M. Cozzarelli⁴

Received 16 April 2013; revised 8 August 2013; accepted 12 August 2013.

[1] The temporal variability observed in redox sensitive species in groundwater can be attributed to coupled hydrological, geochemical, and microbial processes. These controlling processes are typically nonstationary, and distributed across various time scales. Therefore, the purpose of this study is to investigate biogeochemical data sets from a municipal landfill site to identify the dominant modes of variation and determine the physical controls that become significant at different time scales. Data on hydraulic head, specific conductance, $\delta^2\text{H}$, chloride, sulfate, nitrate, and nonvolatile dissolved organic carbon were collected between 1998 and 2000 at three wells at the Norman Landfill site in Norman, OK. Wavelet analysis on this geochemical data set indicates that variations in concentrations of reactive and conservative solutes are strongly coupled to hydrologic variability (water table elevation and precipitation) at 8 month scales, and to individual eco-hydrogeologic framework (such as seasonality of vegetation, surface-groundwater dynamics) at 16 month scales. Apart from hydrologic variations, temporal variability in sulfate concentrations can be associated with different sources (FeS cycling, recharge events) and sinks (uptake by vegetation) depending on the well location and proximity to the leachate plume. Results suggest that nitrate concentrations show multiscale behavior across temporal scales for different well locations, and dominant variability in dissolved organic carbon for a closed municipal landfill can be larger than 2 years due to its decomposition and changing content. A conceptual framework that explains the variability in chemical concentrations at different time scales as a function of hydrologic processes, site-specific interactions, and/or coupled biogeochemical effects is also presented.

Citation: Arora, B., B. P. Mohanty, J. T. McGuire, and I. M. Cozzarelli (2013), Temporal dynamics of biogeochemical processes at the Norman Landfill site, *Water Resour. Res.*, 49, doi:10.1002/wrcr.20484.

1. Introduction

[2] The leaching of reactive contaminants from landfill and waste management sites is controlled by multiple geochemical, hydrological, and microbiological factors, and occurs across various time scales [Christensen *et al.*, 2001; Cozzarelli *et al.*, 2001; Jardine, 2008; Bjerg *et al.*, 2011]. Knowledge about the temporal variability of reactive contaminants in groundwater is important to assess contaminant plume migration, evaluate associated health risks, and

undertake timely action. However, temporal patterns and nonlinear interactions in biogeochemical processes controlling this variability are poorly understood in groundwater systems.

[3] The majority of organic and inorganic contaminants in the subsurface are affected by the hydrological and geochemical properties of the porous media [Mercer, 1983]. Hydrologic variations including water table elevation and precipitation play a pivotal role in the migration and distribution of contaminants in groundwater. For example, Fendorf *et al.* [2010] suggested that the patterns of recharge and discharge of groundwater, especially groundwater pumping and time since recharge, were important factors influencing arsenic concentrations in South and Southeast Asia. The impact of seasonal rainfall events on redox processes at a shallow, sandy aquifer contaminated with petroleum hydrocarbons and chlorinated solvents was addressed by McGuire *et al.* [2000]. They concluded that changes in concentrations of redox-sensitive chemicals appeared to be related to rainfall events at monthly and larger (3 year) time scales. Several other studies have documented the importance of hydrologic controls (changes in direction and seasonality of flow, recharge timing, transition across

¹Department of Biological and Agricultural Engineering, Texas A&M University, College Station, Texas, USA.

²Now at Earth Sciences Division, Lawrence Berkeley National Laboratory, Berkeley, California, USA.

³Department of Geology, University of St. Thomas, St. Paul, Minnesota, USA.

⁴U.S. Geological Survey, Reston, Virginia, USA.

Corresponding author: B. Arora, Earth Sciences Division, Lawrence Berkeley National Laboratory, 1 Cyclotron Rd., MS 74-327R, Berkeley, CA 94720, USA. (email: barora@lbl.gov)

hydrologic boundaries, etc.) on geochemical concentrations at both laboratory column and landfill scales [Mitchell and Branfireun, 2005; Cozzarelli et al., 2011; B. Arora et al., Redox geochemistry within homogeneous and layered soil columns under varying hydrological conditions, submitted to *Water Resources Research*, 2013; D. Hansen et al., Biogeochemical cycling in heterogeneous unsaturated soils: A comparison between live and sterilized sediments, submitted to *Vadose Zone Journal*, 2013]. Topographic and landscape controls such as shifts in vegetation structure and density can also contribute to spatio-temporal dynamics of water content availability and infiltration characteristics of the porous media [Asseng et al., 2001; Raz-Yaseef et al., 2010; Jana and Mohanty, 2012].

[4] Apart from hydrologic variations, geochemical processes are also known to affect redox dynamics in groundwater systems. The progression of redox reactions and subsequent transformation of contaminants is based on thermodynamic energy yields as aerobic respiration, nitrate reduction, manganese reduction, iron reduction, sulfate reduction, and methanogenesis [Chapelle, 2001; Megonigal et al., 2004]. However, heterogeneities in contaminant load (e.g., changes in organic carbon content and metals), aquifer composition (e.g., presence of iron and/or manganese oxides), geologic framework, etc., can result in a departure from the characteristic spatial sequence of redox zones [Champ et al., 1979; Heron and Christensen, 1995; Heron et al., 1998; Christensen et al., 2000; Van Breukelen et al., 2003; Harris et al., 2006]. Redox dynamics can be spatially variable and intensified at the plume fringe, where they are governed by the differences between the composition of the landfill and the mineralogy of the aquifer as well as by seasonal biogeochemical cycling [Kjeldsen et al., 1998; Sinke et al., 1998; McGuire et al., 2002; Scholl et al., 2006; Tuxen et al., 2006]. Apart from being spatially heterogeneous, the distribution of redox species can be temporally variable as many of the redox reactions are microbially mediated. Differences in microbial populations, community structures, and their biotic interactions (e.g., biomass accumulation and competition) can add to the temporal variability of the distribution of contaminants [Röling et al., 2001; Jolley et al., 2003; Haack et al., 2004].

[5] Therefore, the release of contaminants is a function of the complex interactions between physical factors (e.g., porosity, permeability, and dilution), chemical mechanisms (e.g., adsorption, redox, and precipitation), geological controls (e.g., lithologic variations, depositional patterns, and presence of fractured rock), ecological interactions (e.g., type of vegetation and rooting depth), and microbial activities (e.g., biodegradation and biotransformation) [Christensen et al., 2000; Bjerg et al., 2003, 2011; Wanty and Berger, 2006; Pacific et al., 2011]. For example, the progression of redox zones is affected by the supply rate of terminal electron acceptors, which is governed by permeability and hydrologic recharge events, and by the presence of oxidized minerals, which is controlled by the geologic framework of the aquifer [Lovley and Chapelle, 1995; Kamolpornwijit et al., 2003; Mukherjee et al., 2008]. Consequently, microbial activity is influenced by hydrological and geological processes that control the transport of terminal electron acceptors and the distribution

of redox and other reactant species [Hunter et al., 1998; Haack and Bekins, 2000; Geesey and Mitchell, 2008]. In return, microbial processes utilize these reactants and modify the chemical composition of the groundwater. Biotic degradation of organic carbon can change pH and groundwater alkalinity, thus affecting geochemical mechanisms (such as precipitation and sorption), while biomass accumulation can impede flow, thus affecting hydrological variables (such as permeability and aquifer porosity) [Mills et al., 1989; Taylor and Jaffe, 1990; Kusel, 2003]. Therefore, the distribution of redox-sensitive compounds is governed by an aggregation of linked hydrological and biogeochemical processes.

[6] Since these biogeochemical interactions are nonlinear and complex, changes to measured water chemistry parameters (such as pH, SO_4^{2-}) can indicate the influence of multiple processes simultaneously. Moreover, the time frame of analysis is an important factor when considering changes in chemical composition, redox state, microbial community structure, vegetation growth, or other external forcing [Bloschl and Sivapalan, 1995; Langmuir, 1997; Smith, 2007]. Therefore, wavelet analysis is considered to be an apt technique for carrying out this time scale analysis of water chemistry parameters [Kumar and Fofoula-Georgiou, 1997].

[7] Wavelet analysis is a technique that can decompose the data into time and frequency domains simultaneously [Fofoula-Georgiou and Kumar, 1994; Torrence and Compo, 1998]. This time frequency localization property enables wavelet functions to reveal the natural variability of a data set that other techniques miss, such as detecting discontinuities, seasonal trends, and long-term patterns of the data set [Daubechies, 1992; Merry and Steinbuch, 2005; Sang, 2012]. Percival [2008] presents an example of two time series that are difficult to differentiate by simple statistical measures like the sample mean and variance, whereas wavelet analysis can meaningfully differentiate the overall variance structure of the two series. Classical methods like Fourier analysis are also not suitable for analyzing the natural frequencies of biogeochemical data sets as they represent the aggregation of many nonstationary processes [Lau and Weng, 1995; Milne et al., 2009]. Although a relatively new technique, wavelet analysis has been used to extract the dominant frequencies of precipitation and runoff data in the Aegean region of Turkey and highlight the time scale relationship of this rainfall-runoff data [Partal, 2012]. Similarly, wavelets have been implemented to capture vegetation dynamics at a regional scale and associate these with seasonal changes in vegetation phenology [Martinez and Gilbert, 2009]. Zhang et al. [2006] analyzed temporal trends and frequency changes in three major stations of Yangtze River, China, using simple linear regression, Mann–Kendall test, and wavelet transform analysis. They concluded that Mann–Kendall and parametric *t*-test suggest a decreasing trend in the upper Yangtze River, but wavelet analysis reveals that the changes in stream flow are not influenced by a single factor like climatic change, but by multiple factors like destruction of vegetation, land reclamation, and other human activities.

[8] In summary, variations in water chemistry parameters are difficult to interpret as soil hydraulic properties, chemical reactions, microbial composition, and external

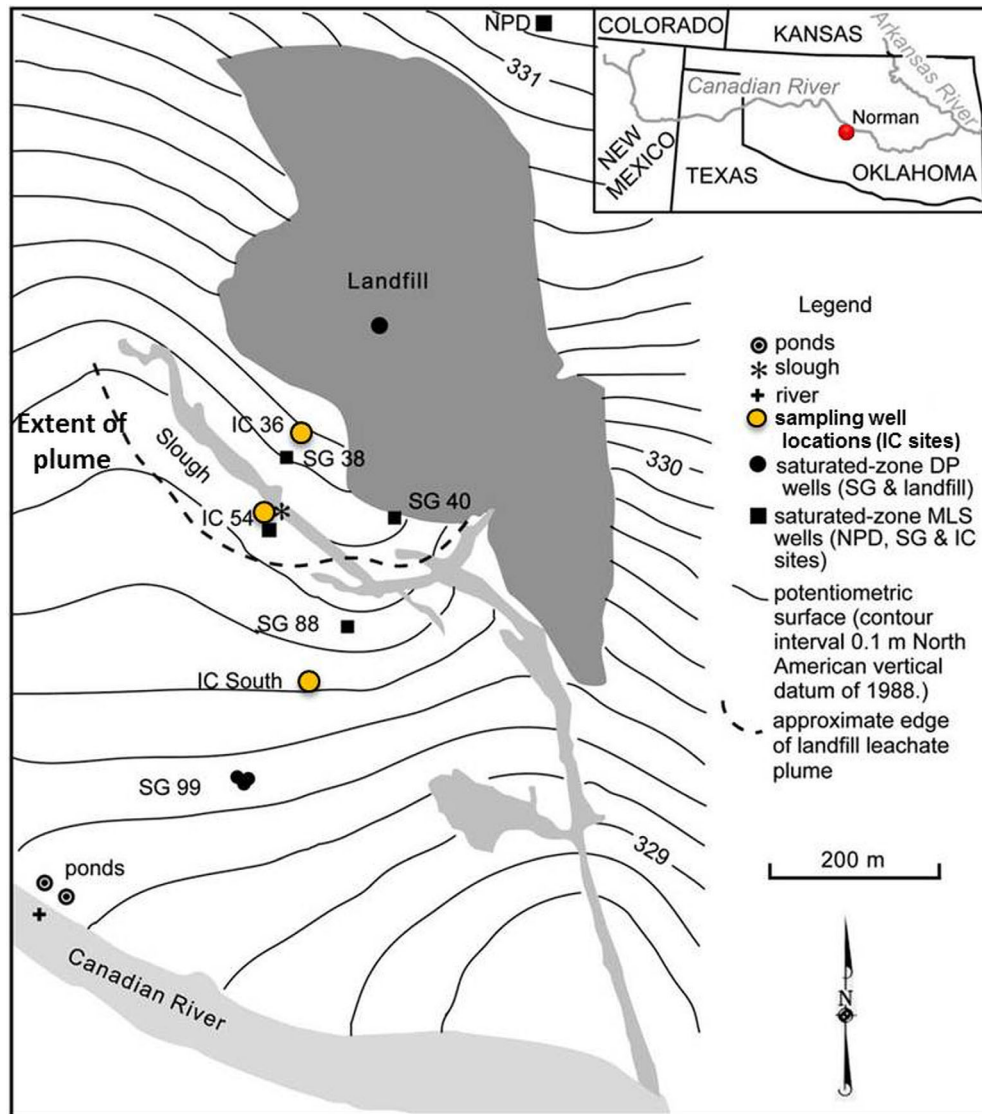


Figure 1. Map depicting the location of the Norman Landfill site and the multilevel sampling wells (IC 36, IC 54, and IC South) overlain on the potentiometric surface.

forcing (such as rainfall events and aquifer withdrawal) change with time. Therefore, this study is an effort to understand the temporal changes in leachate composition and extract their linkages to hydrological and geochemical processes using wavelets. The specific objectives of this study are to (i) extract the natural variability of the biogeochemical data set from a closed municipal landfill site and (ii) identify the dominant processes that attenuate and/or control this temporal distribution of landfill leachate.

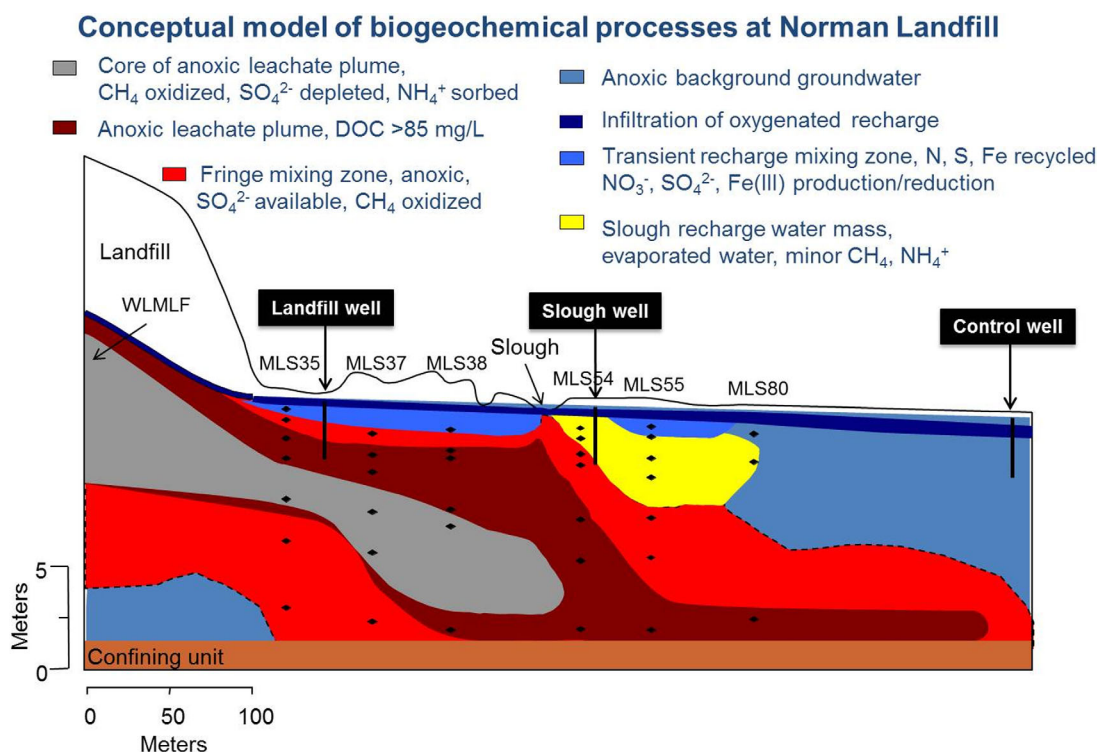
2. Field Procedures

2.1. Site Description

[9] The Norman Landfill is a closed municipal landfill that operated for 63 years in the city of Norman, Oklahoma (Figure 1). By the mid 1990s, the leachate plume from the site extended approximately 250 m downgradient toward the Canadian River [Scholl and Christenson, 1998]. Near the landfill, the groundwater is shallow (about 2 m deep from the land surface) [Scholl *et al.*, 2006; Cozzarelli

et al., 2011]. Previous hydrologic investigations reveal the dynamic nature of the water table with diurnal fluctuations in response to transpiration, observed seasonal variations as large as 1.4 m from winter to summer, and rapid variations in response to rainfall events [Scholl *et al.*, 2005]. The seasonality of the water table position is primarily attributed to rainfall and evapotranspiration. Oklahoma has a continental climate, and the character of rainfall varies with the seasons. On an average, the climatological maximum for rainfall occurs in May and a secondary maximum occurs in September [Comrie and Glenn, 1998]. In their study, Scholl *et al.* [2005] indicated that rainfall events can elevate the water table within 0.6–2 days, and the residence time of the groundwater is on the order of days depending on the season and other recharge events. The riparian zone near the landfill is responsible for water-level decline during the growing season (mid-April to October) [Scholl *et al.*, 2005].

[10] Analyses of groundwater samples have indicated that the leachate also interacts with a former Canadian



River channel, referred to as the slough [Becker, 2002] (Figure 1). The slough is an ephemeral wetland that is an expression of the local water dynamics. Seasonal variations in the slough water depth can be as much as 1 m deep in the spring to dry in summer and occur in response to groundwater and precipitation [Christenson *et al.*, 1999; Lorah *et al.*, 2009]. The slough and the leachate contaminated groundwater are hydrologically connected such that the groundwater discharges into the slough along the northeast bank while the slough recharges the groundwater along the southwest bank [Scholl *et al.*, 2005; Lorah *et al.*, 2009].

[11] The biogeochemistry of the site indicates sulfate reduction, iron reduction, and methanogenesis to be important processes for degradation of organic matter [Cozzarelli *et al.*, 2000; Eganhouse *et al.*, 2001; Grossman *et al.*, 2002]. Báez-Cazull *et al.* [2008] reported that seasonal rainfall patterns were dominant controls on redox zonation, especially for iron and sulfate reduction, while analyzing 3 years of data from the slough. They also concluded that exact temporal controls on the fate of iron could not be determined because of multiple biogeochemical controls. Cozzarelli *et al.* [2011] confirmed that chemical concentrations in the plume boundaries are affected by hydrologic processes at various time scales. Their analysis of the plume-scale data revealed that the upper boundary of the leachate plume is an active redox location, while the center of the plume is depleted in sulfate and has low oxidation capacity. The spatial variability of biogeochemical processes is also evident in the existing conceptual framework

of the Norman Landfill site (Figure 2). Therefore, the Norman Landfill provides an opportunity to study the temporal variability of biogeochemical processes in the leachate plume and identify the physical controls governing contaminant distributions at different locations within the site.

2.2. Data Description

[12] Three multilevel wells located on a transect parallel to the groundwater flow were used to collect the biogeochemical data at the Norman Landfill site (Figure 1). These wells have screens set at different elevations to capture the dynamics of the local water table [Scholl *et al.*, 2006]. The landfill well (IC 36) is located 35 m from the edge of the landfill mound, the slough well (IC 54) is located 7 m south of the slough, and the control well (IC South) is 85 m downgradient from the slough [Breit *et al.*, 2005]. The wells are named as such because the geochemical characteristics of the IC 36 well suggest its interactions with the leachate plume, the IC 54 well with the slough and the leachate plume, and the IC South with background groundwater concentrations or recharged slough water [Breit *et al.*, 2005]. The control well (IC South) is located in an area that was prone to flooding during the 1980s and has sparse vegetation due to the activity of the river channel [Schlotmann, 2001]. In contrast, the vegetation is quite dense near the landfill and slough wells with mature trees and understory [Tuttle *et al.*, 2009]. The differences in geochemical characteristics and hydrologic interactions between the three well locations are evident in Figure 2,

Table 1. Sampling Frequency for Different Wells for Wavelet Analysis

Wells	Analyzed Well Screens	Elevation Based on Center of the Screen (m)	Analyzed Dates (month/year)
Control well (IC South)	5 to 14	327.995 to 329.355	May 1998 to May 2000
Landfill well (IC 36)	7 to 17	328.385 to 329.730	Nov 1998 to May 2000
Slough well (IC 54)	7 to 14	328.265 to 329.230	May 1998 to May 2000

which represents the distinct biogeochemical zones for the wells using the conceptual framework of the Norman Landfill site.

[13] Wavelet analysis was performed on data collected between 1998 and 2000 from the control, landfill, and slough wells (Table 1) [Cozzarelli *et al.*, 2011]. This data set contains hydrological and geochemical indicators including hydraulic head, specific conductance, $\delta^2\text{H}$, bromide, chloride, sulfate, nitrate, and nonvolatile dissolved organic carbon (NVDOC) at all well locations. Monthly data collected at a minimum of eight depth levels for each well resulted in approximately 200 data points for each variable. Specific conductance was measured using a portable meter, anions were analyzed using ion chromatograph, NVDOC concentrations were determined following the method of Qian and Mopper [1996], and isotopic analyses were done by equilibration with gaseous hydrogen for $\delta^2\text{H}$. A more detailed description of the analytical methods can be obtained from Scholl *et al.* [2006].

3. Methods

3.1. Wavelet Analysis

[14] Since groundwater systems are complicated by linked biogeochemical processes, wavelets offer a powerful technique to analyze the observed redox patterns and identify the dominant processes that control water chemistry variations in the temporal domain. Wavelets have the ability to provide high interscale decorrelation especially when the contributing biogeochemical processes are interlinked and have multiscale characteristics [Diou *et al.*, 1999]. Therefore, a wavelet transform is performed on the Norman Landfill data set to obtain a comprehensive view of the frequency variations over time, and a multilevel decomposition (MLD) analysis is conducted to obtain the physical controls governing biogeochemical patterns at different time scales. These techniques are described in the following sections.

3.1.1. Time Frequency Analysis

[15] The wavelet transform is one of the most favored time frequency analysis methods for characterizing multiscale, nonstationary processes across spatial and temporal scales [Shao *et al.*, 2003; Addison, 2005; Das and Mohanty, 2008; Beecham and Chowdhury, 2010]. The continuous wavelet transform (CWT) is obtained by decomposing the data $D(t)$ with a wavelet function $\psi(t)$ and generating wavelet coefficients W that indicate the level of correlation between the wavelet function and the data:

$$W_D(a, b) = \int_{-\infty}^{\infty} \Psi_{a,b}^*(t) D(t) dt \quad (1)$$

where t is time, $*$ denotes the complex conjugate of the wavelet function, and the wavelet function is described by

$$\Psi_{a,b}(t) = \frac{1}{\sqrt{a}} \Psi\left(\frac{t-b}{a}\right), \quad a > 0, \quad -\infty < b < \infty \quad (2)$$

where a is the scale parameter that controls the dilation or contraction, and b is the shift parameter that determines the location of the wavelet. This flexibility of the wavelet to be stretched and translated in both time and frequency domains is useful for identifying localized, intermediate, and long-term patterns existing across different time scales [Kumar and Foufoula-Georgiou, 1997]. The choice of the wavelet function is not arbitrary and must satisfy the basic properties of (i) zero mean $\left(\int_{-\infty}^{\infty} \Psi(t) dt = 0\right)$, (ii) unit energy $\left(\int_{-\infty}^{\infty} \Psi^2(t) dt = 1\right)$, and (iii) conservation of energy during transformation [Daubechies, 1992; Farge, 1992].

[16] A wide variety of wavelet functions exist in the literature and present the advantage of allowing the most appropriate wavelet (irregular, asymmetrical, and other wave shapes) to be chosen for the time series data as opposed to Fourier analysis, which is restricted to revealing the sinusoid features of the data [Addison, 2005; Fugal, 2009]. In this study, Morlet wavelet is used to extract the dominant frequencies within the biogeochemical data set as it has a shape similar to the time series data of the Norman Landfill site. Morlet wavelet is obtained by localizing a complex sine wave with a Gaussian envelope. This wavelet has both complex and real parts and, therefore, enables the identification and fine tuning of significant frequencies [Lau and Weng, 1995; Hariprasath and Mohan, 2009].

3.1.2. Local and Global Wavelet Spectrums

[17] The modulus of the wavelet coefficients is used to develop a continuous-time power spectrum $p_D(a, b)$ defined as:

$$p_D(a, b) = W_D(a, b) W_D^*(a, b) = |W_D(a, b)|^2 \quad (3)$$

[18] This wavelet power spectrum is advantageous as it provides the variance of the time series in both frequency and time domains [Guan *et al.*, 2011]. This local power spectrum can be averaged along the time axis to obtain the global wavelet spectrum [Torrence and Compo, 1998]:

$$\overline{W}^2(a, b) = \frac{1}{N} \sum_{n=0}^{N-1} |W_D(a, b)|^2 \quad (4)$$

where N is the length of the data.

[19] A 5% significance level for the global wavelet spectrum and the confidence interval of the contours in the local power spectrum are determined with a significance testing on the background spectrum. The distribution of the local wavelet power spectrum at each time t and scale a is given as [Torrence and Compo, 1998]:

$$\frac{|W_D(a, b)|^2}{\sigma^2} \Rightarrow \frac{1}{2} P_k \chi^2 \quad (5)$$

where σ^2 is the variance, χ^2 is the chi-square value obtained for the chosen confidence level, and P_k is the mean spectrum at the Fourier frequency k that corresponds to a . For the red-noise background spectrum, P_k is obtained as [Torrence and Compo, 1998; Partial, 2012]:

$$P_k = \frac{1 - \alpha^2}{1 + \alpha^2 - 2\alpha \cos(2\pi k/N)} \quad (6)$$

where α is the assumed lag-1 autocorrelation, and k ($= 0 \dots N/2$) is the frequency index. The lag-1 autocorrelation coefficient is taken here to be 0.72. The confidence intervals for the contour lines of the local wavelet power spectrum are thus obtained by choosing a red-noise background spectrum with a particular confidence (such as 75%, 50%, 25%, and 5%) for χ^2 . A 5% significance level for the global wavelet spectrum is obtained using a white-noise background spectrum. The global wavelet spectrum can also be fitted by a chi-square distribution of the form χ_v^2/v , where the degree of freedom v can be estimated as follows [Torrence and Compo, 1998]:

$$v = 2\sqrt{1 + \left(\frac{t_{avg}\delta t}{\gamma a}\right)} \quad (7)$$

where t_{avg} is the number of points averaged over, δt is the sampling frequency, and γ is the empirically derived decorrelation factor for time averaging. Based on Torrence and Compo [1998], γ is taken here to be 2.32. Wavelet software provided by C. Torrence and G. Compo (<http://atoc.colorado.edu/research/wavelets/>) is used in this study for obtaining the local wavelet power spectrum, the global power distribution, and the confidence intervals.

3.1.3. Wavelet Cross-Spectrum

[20] The physical relationship between two time series in the time frequency domain can be obtained using wavelet cross-spectrum analysis. A wavelet cross-spectrum provides the opportunity to quantify the correlation between the wavelet power spectra of two variables (D_1 , D_2) [Grinsted et al., 2004]:

$$p_{D_1, D_2}(a, b) = W_{D_1}(a, b) W_{D_2}^*(a, b) \quad (8)$$

[21] This wavelet cross-spectrum can be decomposed into modulus $|p_{D_1, D_2}(a, b)|$ and phase angle $\Phi_{D_1, D_2}(a, b)$ as [Maraun and Kurths, 2004]:

$$p_{D_1, D_2}(a, b) = |p_{D_1, D_2}(a, b)| e^{i\Phi_{D_1, D_2}(a, b)} \quad (9)$$

such that the modulus quantifies the power, and phase angle represents the delay in the time-dependent relationship between D_1 and D_2 . For the Norman Landfill data set, it is desirable to know how two nonstationary geochemical variables vary in time.

3.1.4. Multilevel Decomposition

[22] The wavelet decomposition technique, as the name implies, decomposes the original data into a number of fre-

quency bands at discrete levels or time scales. At the first step, the time series data is split into two to reveal the high-pass bandwidth or the detailed components, and the low-pass bandwidth or the approximate components [Misiti et al., 2008; Kia et al., 2009; Quiroz et al., 2011]. Each low-pass bandwidth is further decomposed to obtain the next level of hierarchy. This technique thus provides the opportunity to throw out the noise (detailed components) and retrieve the smoothed trend of the data (approximate components) at each level. The decomposition levels are based on the total number of data points and the sampling frequency [Mallat, 1999].

[23] The hierarchical details and approximations are obtained by iteratively applying a high-pass filter and an associated low-pass filter, which must satisfy certain conditions including orthonormality [Labat et al., 2000; Percival and Walden, 2000]. In the wavelet analysis, a wavelet function $\psi(t)$ constitutes the high-pass filter, and its scaling function $\phi(t)$ forms the low-pass filter. The choice of the wavelet function is such that it is orthogonal to both translates and dilates, while the scaling function is only orthogonal to the translates [Kumar and Foufoula-Georgiou, 1997]. The detail (D_m) and approximation (A_m) components at any decomposition level m are thus given by:

$$D_m(t) = \sum_{k=-\infty}^{\infty} W(m, k) \psi_{m, k}(t) \quad (10)$$

$$A_m(t) = \sum_{k=-\infty}^{\infty} S(m, k) \phi_{m, k}(t) \quad (11)$$

where, k is a discrete location index, and S are the scaling coefficients analogous to the wavelet coefficients. In multi-level decomposition (MLD), a discretized version of equation (1) is used where the wavelet function is scaled by powers of two such that $a = 2^m$ and shifted by integers such that $b = k2^m$ [Martinez and Gilabert, 2009].

[24] In this study, the wavelet decomposition is carried out using the Daubechies 5 (Db5) wavelet and scaling functions, which satisfy the orthogonality requirement. Figure 3 illustrates the shape of the Db5 wavelet and scaling functions and the four levels of decomposition obtained from them. The hierarchical approximations and details $\{(a_1, d_1), (a_2, d_2), (a_3, d_3), (a_4, d_4)\}$ follow dyadic sampling (powers of two) to capture the natural frequencies within the biogeochemical data at 2, 4, 8, and 16 month scales, respectively. Although seasonal variability is usually observed at 1, 3, 6, and 12 month scales, these dyadic decomposition levels still present an opportunity to investigate the event-scale, intra-annual, and biannual trends observed in the Norman Landfill data set.

4. Results and Discussion

[25] Wavelet analysis is used in this study to obtain the dominant variations in the biogeochemical data set and identify the different processes that control these variations at dominant time scales. This section demonstrates the use of continuous and discrete wavelet techniques described in the previous section to investigate the time series behavior

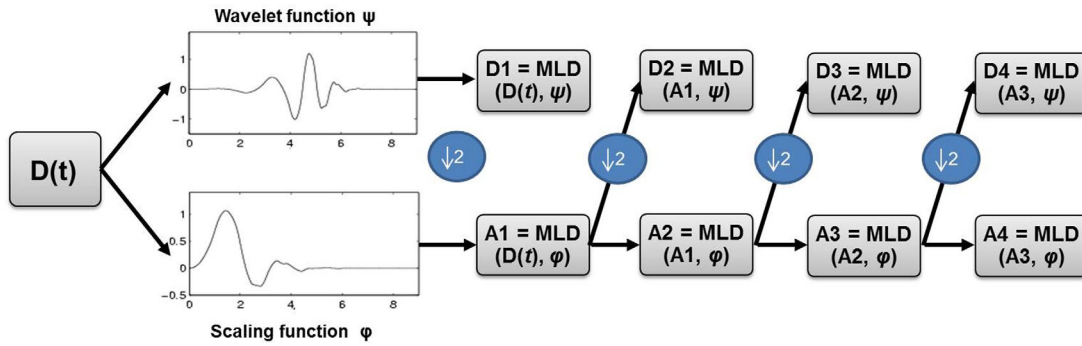


Figure 3. Scheme of the multilevel decomposition (MLD) using Db5 wavelet and scaling functions. $\downarrow 2$ represents the decomposition by a power of two.

of geochemical variables at the control, landfill, and slough wells.

4.1. Temporal Variations and Governing Processes at the Control Well

[26] Figure 4 depicts the temporal characteristics of chloride, sulfate, and bromide at the control (IC South) well

from May 1998 to May 2000. As described in the previous section, Morlet wavelet is employed to study the temporal variations in the data set. The edge effects of time frequency analysis, represented by the cone of influence (indicated by cross-hatched regions in the continuous wavelet spectrum) are excluded from this analysis [Guan et al., 2011]. Based on the Morlet wavelet, all three time series

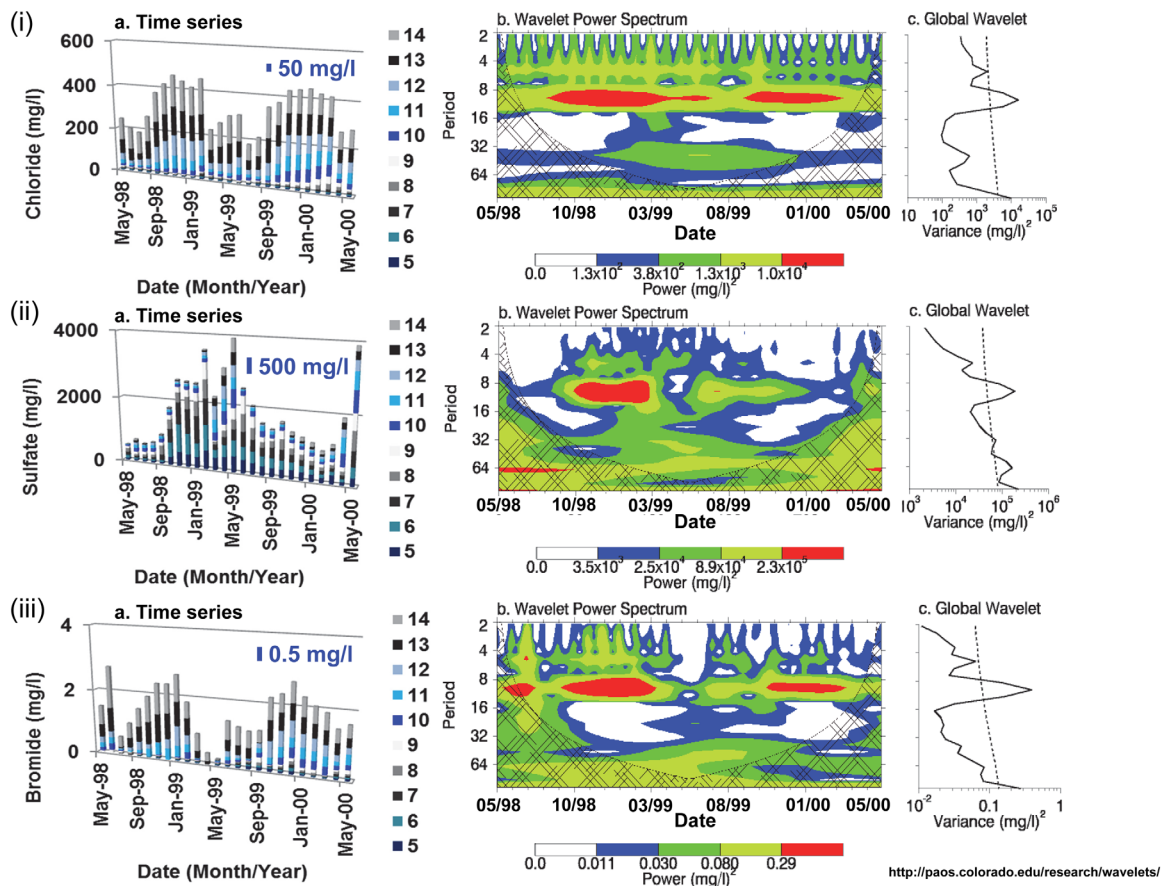


Figure 4. Time frequency analysis at the control well for (i) chloride, (ii) sulfate, and (iii) bromide data displaying time record, continuous wavelet spectrum, and global wavelet spectrum. In the time series graphs, the thickness of the cylinder signifies the concentration value, and the colors represent the well screens 5–14. In the wavelet power spectrum, the cross-hatched regions signify the cone of influence, the contour levels are chosen so that 75%, 50%, 25%, and 5% of the wavelet power is above each level, respectively, and the color bar signifies the strength of power in the wavelet spectrum. In the global wavelet spectrum, dashed line is the 5% significance level using a white-noise background spectrum.

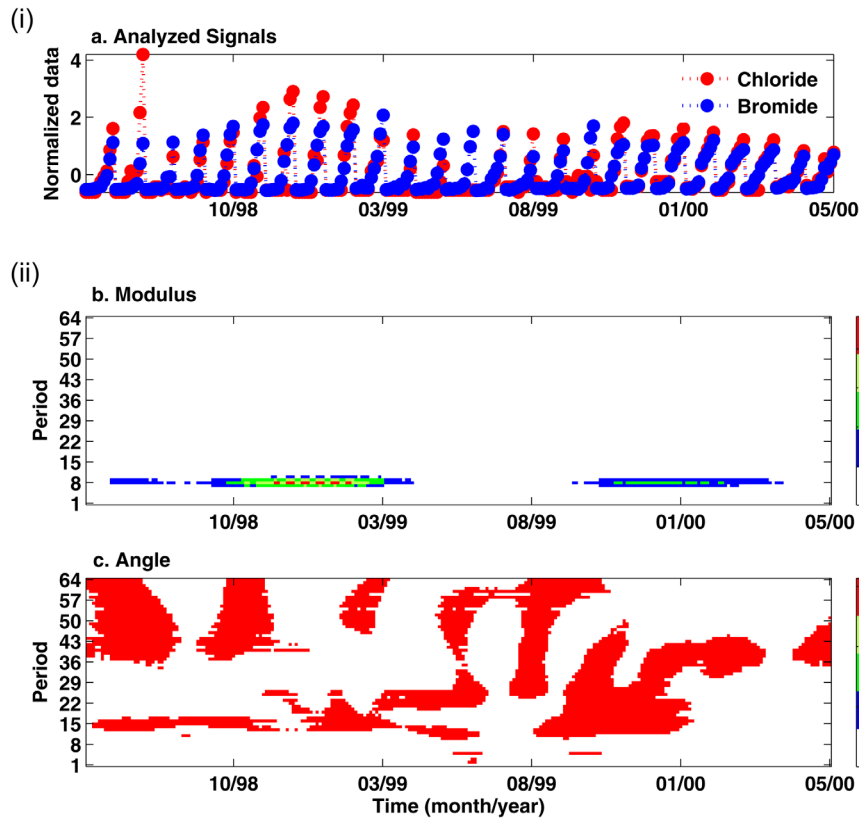


Figure 5. Cross wavelet analysis of bromide and chloride signals at the control well from May 1998 to May 2000: (i) time records of normalized bromide and chloride data and (ii) modulus and angle of the wavelet cross-spectrum.

depict a single dominant scale close to the 12 month period as represented by red contours in their wavelet power spectra (Figure 4b). These red contours are statistically significant at the 75% confidence level based on the background spectrum. This dominant frequency is also evident in the global wavelet spectrum (Figure 4c) for all three geochemical variables at the 5% significance level despite the large differences in their temporal data set (Figure 4a). There is however a discontinuity in the dominant frequency (red contours) at different times for the three variables, with chloride displaying this discontinuity between August and September 1999, bromide between April and November 1999, and sulfate beyond April 1999 in Figure 4b. The reasons for this temporal disparity will be explored using MLD analysis. Another interesting feature in the wavelet power spectra is the small-scale behavior that shows consistent patterns (contours with 50% confidence level) at a 4 month period for chloride data, and somewhat repetitive behavior for bromide data. Since chloride and bromide act mainly as conservative indicators of water flow, these small scale patterns could be representative of seasonal hydrologic events.

[27] The cross wavelet transform is used in this study to describe the physical relationships between bromide and chloride data in the time frequency space. Figure 5a clearly indicates that bromide and chloride data are significantly correlated with each other at the control well. The modulus of the cross wavelet transform further suggests that both signals have significant correlation around scale 8 except in

the interval between April and October 1999, which reveals the quasi-periodic nature of this correlation (Figure 5b). The angle plot (Figure 5c) of the normalized data reveals that the phase lag behavior of the two signals is not consistent throughout the data set. A clear indication of this phase lag behavior and the relative phase difference between the two signals can be obtained from wavelet coherence analysis (not shown here) [Grinsted *et al.*, 2004]. The angle plot (Figure 5c) again suggests the time-localized correlation between bromide and chloride, which could be attributed to similar (conservative) transport behavior but different sources that augment bromide and chloride concentrations at the landfill site. As both signals are conservative indicators of water flow, results pertaining to bromide only will be described.

[28] To further analyze and temporally isolate the processes affecting these dominant frequencies, a multilevel decomposition is performed on the bromide and sulfate data using Db5 wavelet (Figure 6). As mentioned in the previous section, this filtering removes the noise (detailed components) from the data and keeps only the approximations at each scale. The approximations reveal the smoothed trend in the bromide data and are therefore compared with water table elevation and rainfall data to further isolate and identify the hydrologic processes affecting bromide time series (Figure 6(i)). Figure 6(i) illustrates that monthly precipitation events exceeding a certain limit act as discrete episodes that correspond to the “approximation” of bromide at 8 months (a_3). For example, each of the

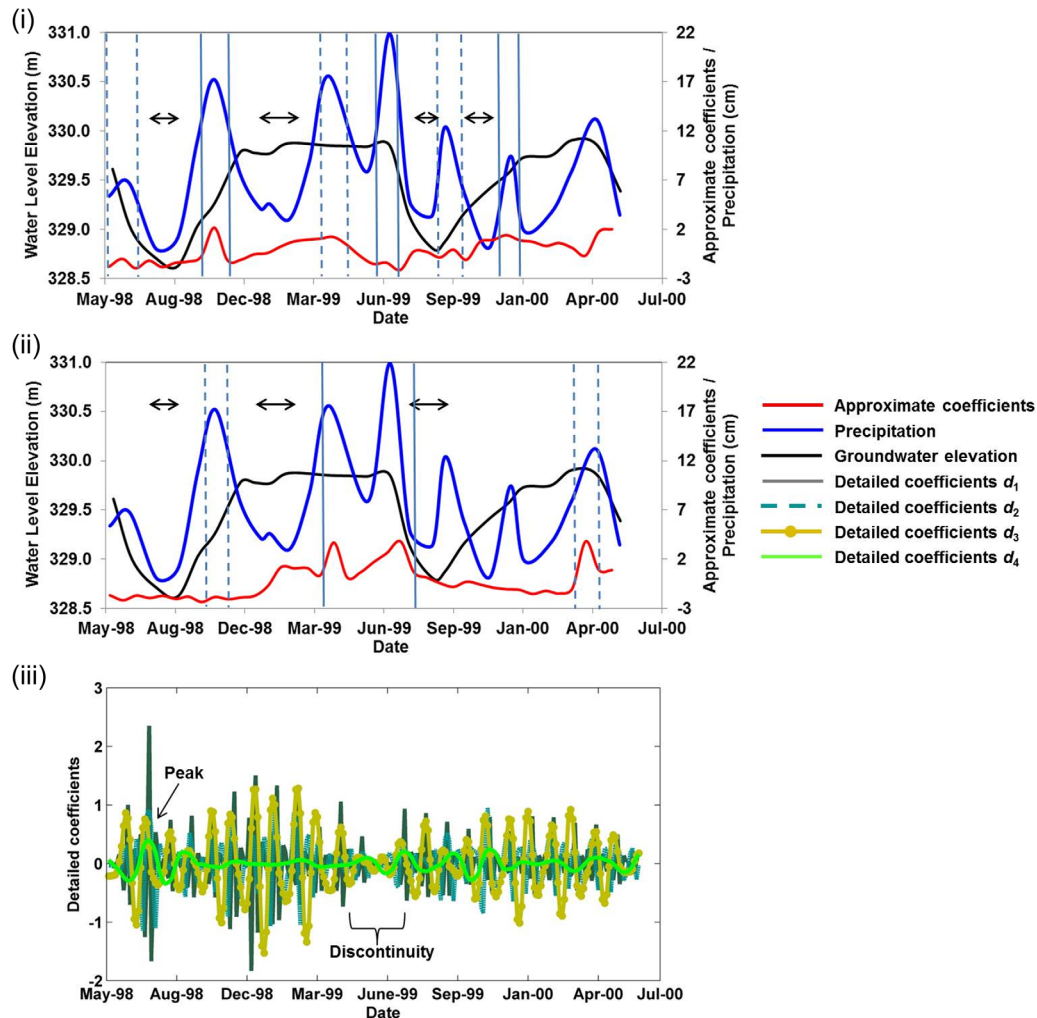


Figure 6. Multilevel decomposition of (i) bromide and (ii) sulfate data at the control well displaying approximate coefficients at 8 months, monthly groundwater elevation, and precipitation record, and (iii) detailed coefficients of bromide at dyadic scales of 2 (d_1), 4 (d_2), 8 (d_3), and 16 (d_4). Two consecutive dashed/solid lines show trends matching between the approximate signal and the precipitation data, and arrows show trends matching between the approximate signal and groundwater elevation data.

rainfall peaks in May 1998, September–October 1998, June 1999, and September 1999 are clearly discernible as humps in the “approximation” of bromide. The smaller mounds in March and December 1999 in the approximation profile also correspond to precipitation events (indicated by lines in Figure 6(i)). These rainfall peaks are significantly correlated with bromide approximation (correlation coefficient = 0.54) at the 90% confidence level. A significant portion of these temporal trends are also associated with water table elevation data (indicated by arrows in Figure 6(ii)) with moderate correlation (correlation coefficient = 0.50). In particular, the dip observed in July–August 1998 and August 1999 in the approximate coefficients of bromide corresponds to groundwater decline in these months, and the slight increase in groundwater table in January and December 1999 is also captured by the approximation profile. The detailed components at four levels of decomposition in Figure 6(iii) reveal frequency-specific behavior, and the d_4 component reveals a peak around July 1998 that coincides with a water table elevation that falls

below a certain limit (Figure 6(i)). The groundwater data in Figure 6(i) also indicates that the summer was relatively dry for 1998 (lowest water level elevation = 328.6 m) as compared to 1999 (lowest water level elevation = 328.8 m). As suggested earlier, this MLD technique provides increasingly finer details at each scale. The detailed components (d_1 – d_3) further confirm the discontinuity in dominant frequency as suggested by the continuous wavelet spectrum. The annual periodic component in the bromide time series is therefore replaced by 5–7 month components that correspond to hydrologic data. Therefore, rainfall recharge events and seasonal variability of the groundwater table affect wavelet coefficients at semiannual scales (~ 8 months) and can be associated with the temporal dynamics of bromide concentrations at the control well.

[29] A multilevel decomposition is also performed on sulfate data to identify the governing processes controlling its temporal variability at the control well. Previous studies have identified several sources of sulfate at the landfill site (such as organosulfur compounds, mineral weathering from

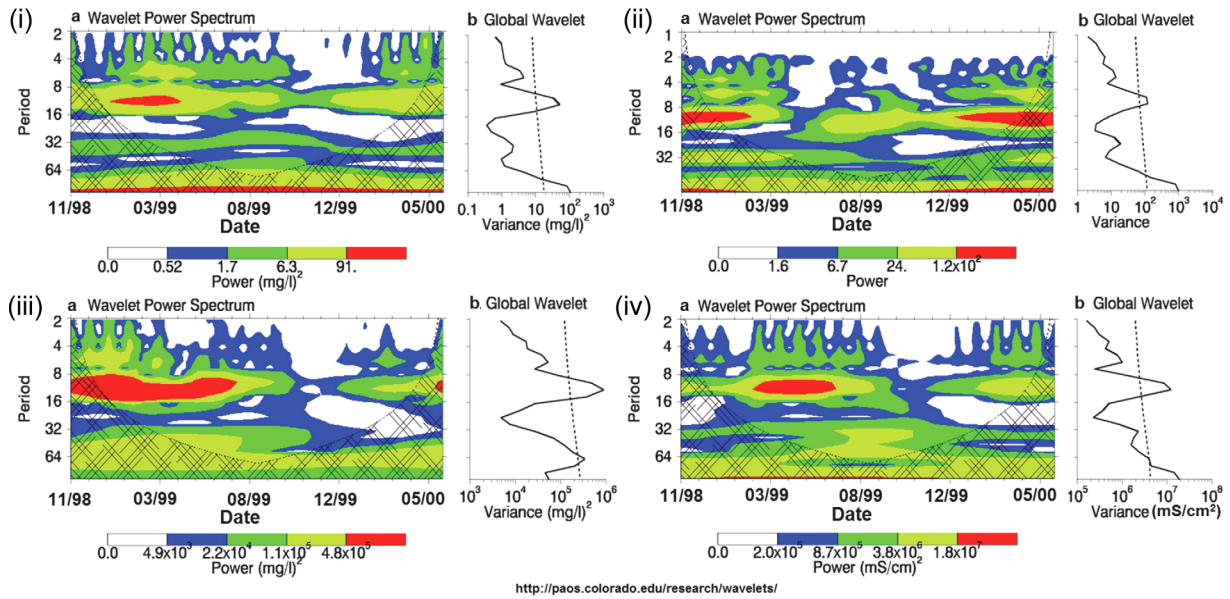


Figure 7. Time frequency analysis at the landfill well for (i) bromide, (ii) $\delta^2\text{H}$, (iii) sulfate, and (iv) specific conductivity data displaying continuous power spectrum and global wavelet spectrum. The cross-hatched regions in the wavelet power spectrum signify the cone of influence, the contour levels are chosen so that 75%, 50%, 25%, and 5% of the wavelet power is above each level, respectively, and the color bar signifies the strength of power in the wavelet spectrum. In the global wavelet spectrum, dashed line is the 5% significance level using a white-noise background spectrum.

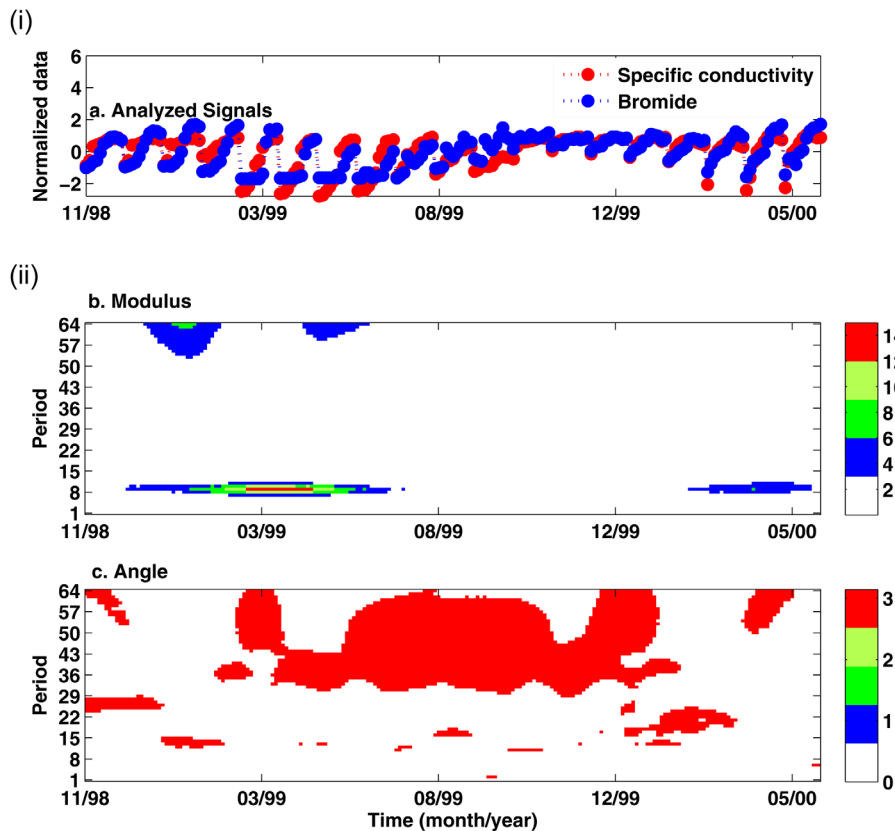


Figure 8. Cross wavelet analysis of bromide and specific conductivity signals at the landfill well from November 1998 to May 2000: (i) time records of normalized specific conductivity and bromide data and (ii) modulus and angle of the wavelet cross-spectrum.

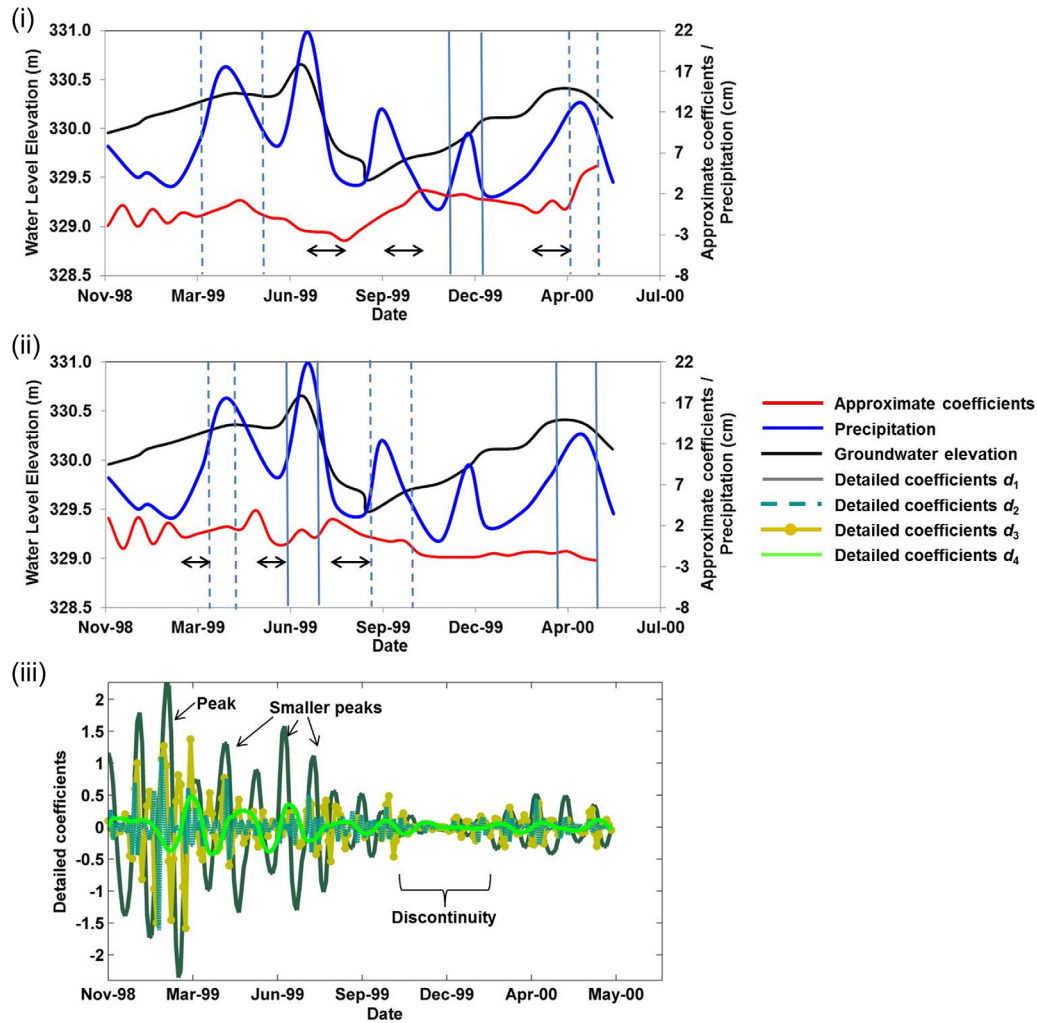


Figure 9. Multilevel decomposition of (i) bromide and (ii) sulfate data at the landfill well displaying approximate coefficients at 8 months, monthly groundwater elevation, and precipitation record, and (iii) detailed coefficients of sulfate at dyadic scales of 2 (d_1), 4 (d_2), 8 (d_3), and 16 (d_4). Two consecutive dashed/solid lines show trends matching between the approximate signal and the precipitation data, and arrows show trends matching between the approximate signal and groundwater elevation data.

barite, pyrite, iron oxide minerals, etc.) and demonstrated the influence of recharge events on sulfur cycling and its transport to deeper depths [Scholl *et al.*, 2006; Tuttle *et al.*, 2009]. However, this study compares the approximations at the scale of the dominant frequency ($a_3 = 8$ months) and hydrologic data to reveal the temporal dynamics of processes controlling sulfate concentrations at the control well (Figure 6(ii)). As expected, there are striking similarities between the seasonal groundwater variations (indicated by arrows) and rainfall events (indicated by lines) with trends in sulfate data. The rainfall events in September 1998, March–June 1999, and April 2000 are evident as humps in the “approximation” of sulfate. The decline in groundwater in July–August 1998 and 1999 and the slight increase in January 1999 is again visible in the sulfate data. Both groundwater variations (correlation coefficient = 0.55) and rainfall events (correlation coefficient = 0.45) show moderate correlations with sulfate “approximation” at 8 month scales at the 90% confidence level. Notice the low levels of sulfate concentrations observed following a rainfall event

even with an increasing water table elevation such as October–November 1998 and 1999, and January 2000. This decrease in sulfate concentrations is attributed to dilution and sulfate reduction processes at the control well [Scholl *et al.*, 2006]. The detailed component d_4 (not shown here) further confirms this decrease in sulfate concentrations following the rainfall events of September 1998 and 1999.

[30] In summary, temporal variations in bromide and sulfate data at the control well show annual periodicity (~ 12 month) and are significantly dominated by water table variability and precipitation events. The temporal anomalies at the dominant scale of variation are related to hydrologic variability for bromide and hydrologic and sulfate reduction processes for sulfate.

4.2. Temporal Variations and Governing Processes at the Landfill Well

[31] Figure 7 represents the temporal dynamics of bromide, $\delta^2\text{H}$, sulfate, and specific conductivity at the landfill (IC 36) well from November 1998 to May 2000. An annual

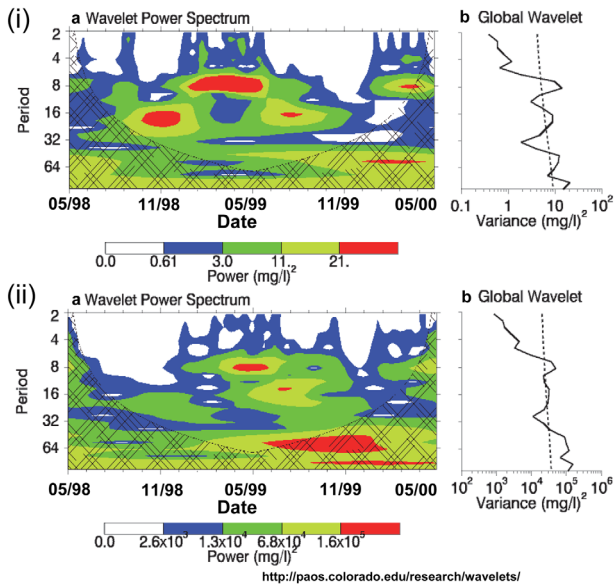


Figure 10. Time frequency analysis at the slough well for (i) bromide and (ii) sulfate data displaying continuous power spectrum and global wavelet spectrum. The cross-hatched regions in the wavelet power spectrum signify the cone of influence, the contour levels are chosen so that 75%, 50%, 25%, and 5% of the wavelet power is above each level, respectively, and the color bar signifies the strength of power in the wavelet spectrum. In the global wavelet spectrum, dashed line is the 5% significance level using a white-noise background spectrum.

periodic component is again visible in the wavelet spectra for all four time series data as denoted by the red contours with 75% confidence level (Figure 7a). This annual component also shows dominance at the 5% significance level (indicated by dashed lines in Figure 7b) in the global wavelet spectra. These periodic structures show time localization and disappear beyond April 1999 for bromide, beyond July 1999 for sulfate and specific conductivity, and show temporal irregularity in $\delta^2\text{H}$ data. These annual components are therefore replaced by 4 month components for bromide and specific conductivity, and a 7 month component for sulfate. Regarding the small scales (2–4 months), repetitive structures (contours with 50% confidence level) are again visible for bromide, $\delta^2\text{H}$, and sulfate time series but not for specific conductivity. Since these variables have different contributing processes, the temporal discrepancies present in the wavelet power spectrum for each signal are different.

[32] Wavelet cross spectrum analysis conducted on bromide and specific conductivity is illustrated in Figure 8. Figure 8a suggests that bromide and specific conductivity signals at the landfill well are significantly correlated with each other. Figure 8b reveals strong correlations at the dominant scale of variation (scale 8). The modulus of correlation at higher time periods (50–64 months) can be ignored in this analysis. The angle plot (Figure 8c) as well as wavelet coherence analysis (not shown here) again reveal that the phase lag behavior is not consistent throughout the data set, thereby suggesting a time-varying correlation between the two signals. Similarly, wavelet cross spectrum analysis suggests a high correlation between bro-

midite and $\delta^2\text{H}$ signals in displaying the periodic annual component (not shown here). As a result, a multilevel decomposition is performed only with respect to bromide and sulfate at the landfill well.

[33] After removing the noise components, the “approximation” of bromide is again compared with hydrologic variations at the landfill well (Figure 9(i)). The rainfall peaks (indicated by lines) in April and December 1999 are clearly evident in the approximation profile of bromide. The rainfall event in April 2000 also coincides with an increase in bromide content. A decrease in water table (indicated by arrows) in July–August 1999 and an increase in October 1999 and March 2000 are also well represented by the approximate coefficients. Apart from November–February time frames for both 1998–1999 and 1999–2000 years, the approximate coefficients of bromide show considerable matching with groundwater table (correlation coefficient = 0.64) and rainfall data (correlation coefficient = 0.44) at the 90% confidence level. Since the region around the landfill well is densely vegetated, a decrease in evapotranspiration processes observed during the winter months seems to be contributing to variations in bromide transport processes during these time frames. Scholl *et al.* [2005] estimated evapotranspiration rates using diurnal water table fluctuations and reported that transpiration had a considerable effect on the water table during the July–October time period. Therefore, a comprehensive analysis of the hydrologic interactions including evapotranspiration losses at the landfill well is able to explain the variability in bromide concentrations at this location.

[34] The “approximation” component of sulfate at the dominant scale of variation ($a_3 = 8$ months) is also compared with hydrologic fluctuations (Figure 9(ii)). These groundwater variations (correlation coefficient = 0.59) and rainfall peaks (correlation coefficient = 0.45) are again found to be moderately correlated with approximate coefficients of sulfate at the 90% confidence level. The rainfall peaks in April 1999, June 1999, September 1999, and April 2000 are visible as humps in the approximation profile of sulfate. The water table rise in March 1999 and decline in May and July 1999 are also captured by the “approximation” of sulfate at 8 month scales. Again, the November–February time frames for both 1998–1999 and 1999–2000 years show poor matching. The trend analysis also reveals a mismatch with a peak in sulfate concentrations around July 1999. Therefore, scale decomposition with all detailed components of sulfate time series is illustrated in Figure 9(iii). The decomposition in the details of sulfate concentrations at the landfill well leads to the identification of three components with very different behaviors. First, a large peak is located around January 1999; second, several smaller peaks are located around December 1998, March, June, and July of 1999, and third, a discontinuity is observed around November 1999 to March 2000 in the d_1 component. The d_2 component also reveals an amplitude reduction in sulfate frequency from November 1998 to March 1999 to the rest of the time series. These detailed components suggest that large peaks in sulfate concentrations in the beginning time frame (November 1998 to March 1999) correspond to a large reoxidation event that possibly led to the dissolution of aquifer solids (barite, iron

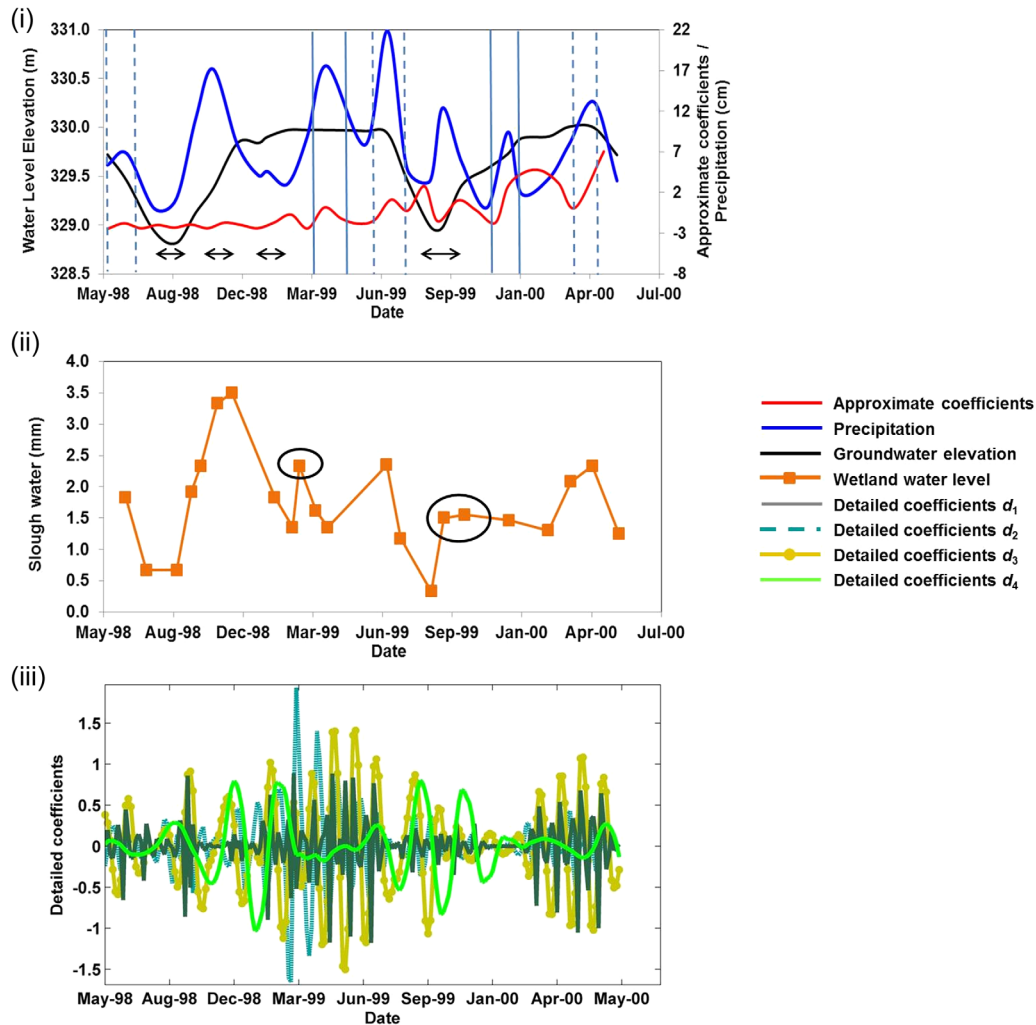


Figure 11. Multilevel decomposition of (i) bromide data at the slough well displaying approximate coefficients at 8 months, monthly groundwater elevation, and precipitation record, (ii) time record of wetland water level (modified from Scholl *et al.* [2005]), and (iii) detailed coefficients of bromide at dyadic scales of 2 (d_1), 4 (d_2), 8 (d_3), and 16 (d_4). Two consecutive dashed/solid lines show trends matching between the approximate signal and the precipitation data, arrows show trends matching between the approximate signal and groundwater elevation data, and ovals represent matching between the approximate signal and wetland water level.

sulfide minerals) because such high sulfate concentrations cannot be attributed to background groundwater or rainfall alone or that the aggregation of various processes (rainfall recharge, vegetative decay, mineral dissolution, etc.) simultaneously resulted in such an event [Schlottmann, 2001]. Previous studies have documented the importance of barite dissolution and its influence on sulfate concentrations at the landfill site [Tuttle *et al.*, 2009; Cozzarelli *et al.*, 2011]. Also, these larger peaks occur immediately following low sulfate concentrations, and several factors (water table variations, undersaturation with respect to sulfate due to increased sulfate reduction and/or iron sulfide formation, etc.) can contribute to an increase in the dissolution rate [Ulrich *et al.*, 2003; Cozzarelli *et al.*, 2011]. The smaller peaks that are spread across different times indicate an increase in sulfate concentrations in response to rainfall events or sulfur cycling as a result of reoxidation of iron sulfide minerals with an increase in groundwater table

[Ulrich *et al.*, 2003; Báez-Cazull *et al.*, 2008]. This sulfur cycling also constitutes a sulfate reduction step, which is visible as the decrease in sulfate concentrations (in addition to dilution) immediately following a rainfall event (Figure 9(ii)). The discontinuity around November 1999 to March 2000 constitutes a significant decrease in sulfate concentrations (greater than those observed for November 1998 to March 1999) and may stem from strong vegetation dynamics at the site. Uptake of sulfate by plant roots is an important process near the landfill well [Tuttle *et al.*, 2009], and this frequency may be reduced during the winter months. This study confirms previous investigations by Scholl *et al.* [2006] that isotopically traced the vertical transport of recharge water for a single rain event of September 1998 and indicated that sulfur redox processes in the top 2 m of the site are associated with recharge events and seasonal patterns of groundwater. Thus, this study does not provide a new conceptual framework for sulfur redox cycling but

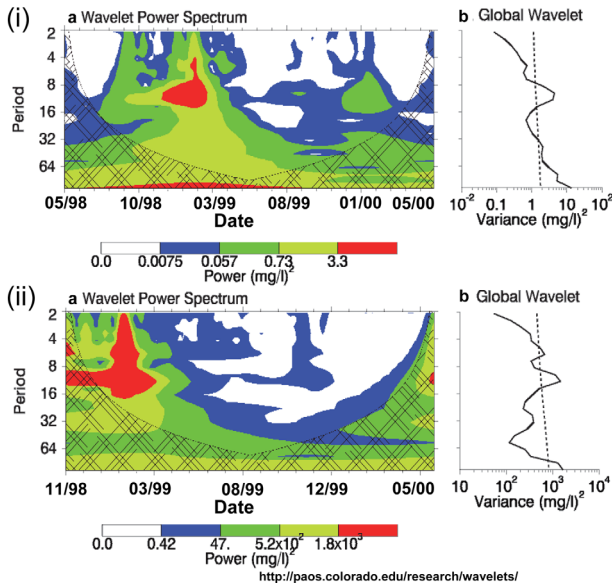


Figure 12. Time frequency analysis of nitrate at the (i) control and (ii) landfill wells displaying continuous power spectrum and global wavelet spectrum. The cross-hatched regions in the wavelet power spectrum signify the cone of influence, the contour levels are chosen so that 75%, 50%, 25%, and 5% of the wavelet power is above each level, respectively, and the color bar signifies the strength of power in the wavelet spectrum. In the global wavelet spectrum, the dashed line is the 5% significance level using a white-noise background spectrum.

provides a clear temporal breakdown of the processes that become significant at different times using wavelet analysis.

[35] In summary, an annual periodic component again dominates different geochemical concentrations at the landfill well. The temporal patterns of geochemical variables are strongly guided by hydrologic variations and affected by vegetation dynamics in the winter months. The multilevel decomposition of sulfate reveals sources (FeS cycling, rainfall events, and increased barite dissolution rate) and sinks (uptake by plant roots) of sulfate at different time frames between November 1998 and May 2000.

4.3. Temporal Variations and Governing Processes at the Slough Well

[36] Figure 10 demonstrates the temporal evolution of bromide and sulfate at the slough (IC 54) well. The wavelet power spectra (Figure 10a) reveal two dominant scales of variation with annual and biannual periodic components for both signals. Both the annual and biannual components are statistically significant at 75% confidence level in the continuous wavelet spectra (indicated by red contours in Figure 10a) and show dominance at the 95% confidence level in the global wavelet spectra (indicated by dashed lines in Figure 10b). Notice that the smaller scales contain negligible power (indicated by white contours in Figure 10a) for both time series. The red contours depicting the annual component (~ 12 months) are discontinuous and replaced by a 2 month component for sulfate and a 5 month component for bromide that reappears in the last phase of

the time series. The biannual component (~ 20 months) also shows time localization and is replaced by a 1–2 month component for bromide and a 2 month component for sulfate.

[37] To further evaluate the processes affecting temporal variability at the slough well, a multilevel decomposition is conducted on the bromide time series. This trend analysis (Figure 11(i)) at the semiannual scale (8 months) portrays significant matching with rainfall data (indicated by lines) in the second year of analysis (April 1999 to May 2000) as well as with a rainfall peak in May 1998. In the first year of analysis (August 1998 to January 1999) as well as in August 1999, there are discrete patterns of decreasing and increasing water table elevation (indicated by arrows) that match with the normalized “approximation” of bromide. A moderate correlation is obtained between the approximate coefficients of bromide and rainfall (correlation coefficient = 0.49) as well as with water elevation data (correlation coefficient = 0.42) at the 90% confidence level. The mismatch between the smoothed “approximation” and hydrologic data can be explained by groundwater-surface water interactions between the wetland and the slough well (Figure 11(ii)). Notice the peak in the normalized bromide signal around February and September 1999 (Figure 11(i)) that matches with the increase in wetland water levels (represented by ovals in Figure 11(ii)). The detailed components d_1 – d_3 (Figure 11(iii)) also identify a frequency around March–July 1999 that is visible in the last phase of the time series as well and corresponds to an increase in wetland water level during the spring season [Scholl *et al.*, 2005]. The d_4 component reveals another frequency that is localized around October–November 1998 and October 1999. This biannual component is reflective of the end of the growing season. The withdrawal of water from the water table by vegetation affects hydrologic dynamics at the site and consequently alters transport of conservative indicators. Previous investigations also corroborate this interpretation [Scholl *et al.*, 2006; Tuttle *et al.*, 2009; Cozzarelli *et al.*, 2011].

[38] In summary, the wavelet spectra for bromide and sulfate at the slough well reveal two frequencies that are more or less localized in time. The annual periodic component in the signal corresponds to slough interactions and showcases a 5 month component (March–July), while the biannual component is a function of vegetation dynamics at the slough well and showcases a 1–2 month component (October–November).

4.4. Exceptions to the Dominant Frequency Rule

[39] There are two exceptions to the dominant scales of variation obtained for the geochemical variables at the control (scale 8), landfill (scale 8), and slough wells (scales 8 and 16). First, nitrate data are inherently multiscale, and this is demonstrated in Figure 12. The wavelet power spectra of nitrate time series (Figure 12a) reveal high power wavelet coefficients (indicated by red contours) across scales 4–16 for the control well and across scales 2–16 for the landfill well. The global wavelet spectra (Figure 12b) also suggest power to be distributed across multiple scales at the 95% confidence interval (indicated by dashed lines). This clearly indicates that different processes with different frequency ranges are contributing to the total wavelet

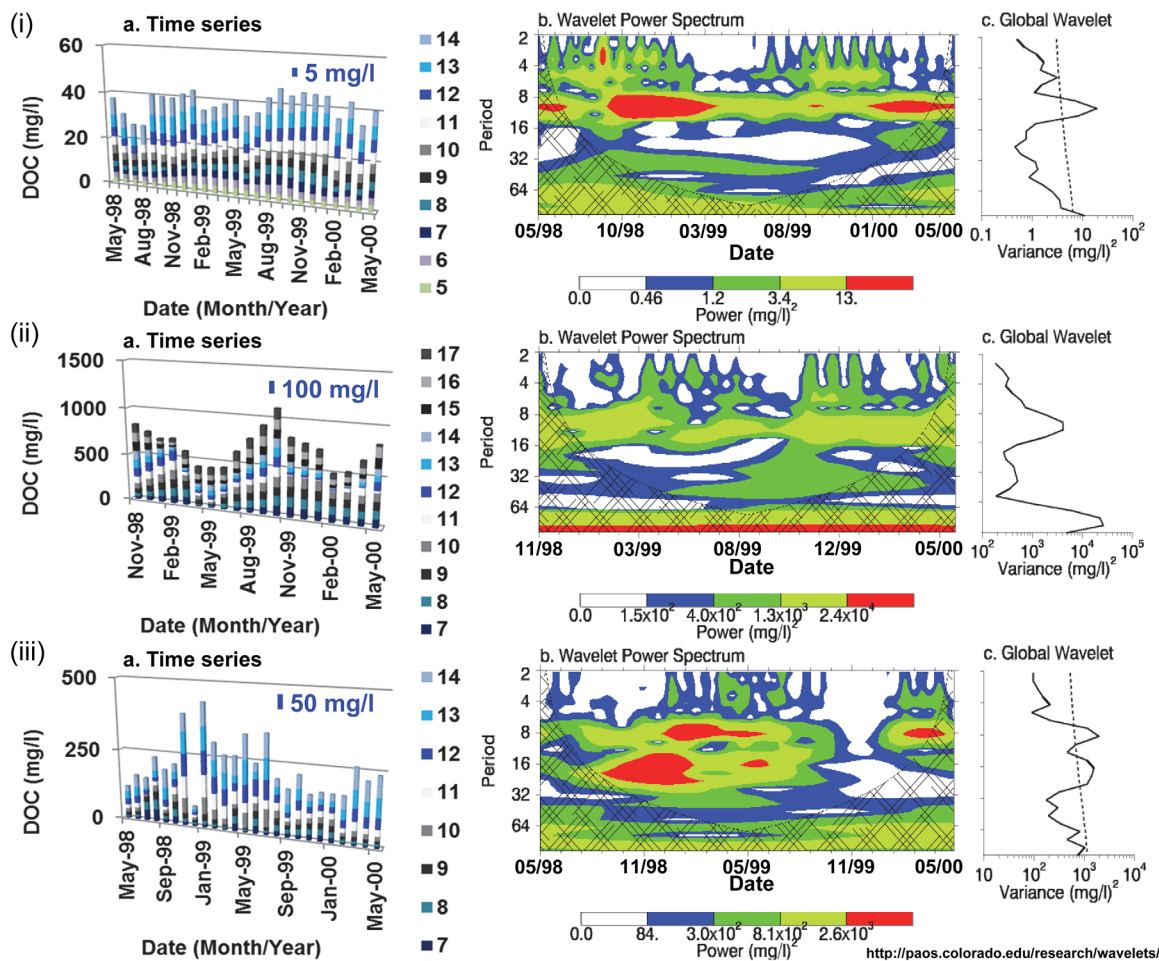


Figure 13. Time frequency analysis of DOC at the (i) control, (ii) landfill, and (iii) slough wells displaying time series data, continuous power spectrum, and global wavelet spectrum. In the time series graphs, the thickness of the cylinder signifies the concentration value, and the colors represent the well screens. In the wavelet power spectrum, the cross-hatched regions signify the cone of influence, the contour levels are chosen so that 75%, 50%, 25%, and 5% of the wavelet power is above each level, respectively, and the color bar signifies the strength of power in the wavelet spectrum. In the global wavelet spectrum, the dashed line is the 5% significance level using a white-noise background spectrum.

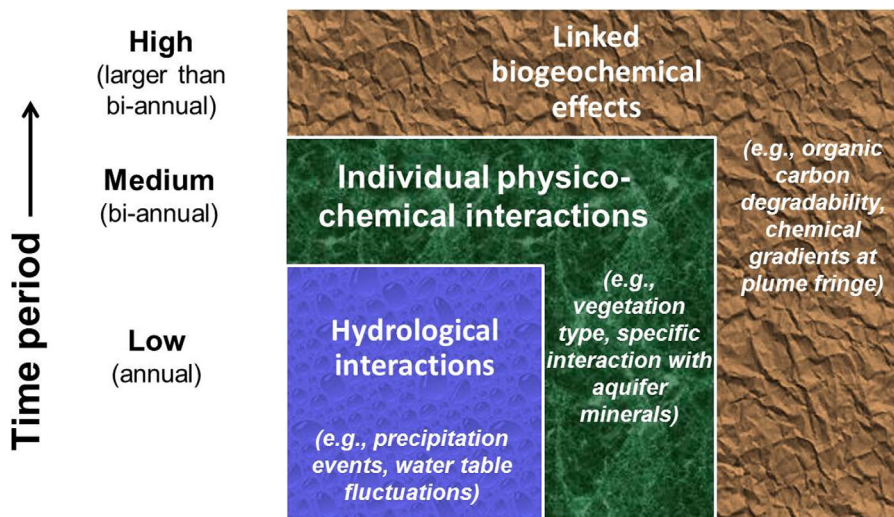


Figure 14. Conceptual diagram showing the governing controls of redox geochemistry at increasing time scales.

spectra. Notice that the regions of significant power are limited to November 1998 to March 1999 for both wells. The dominant variability in nitrate concentrations during these winter months could be a result of several concomitant processes such as external climate forcing (e.g., snow storms), plant decay, and bacterial decomposition of stored nitrogen, which occurred during a similar time frame of November–March for both wells.

[40] Second, dissolved organic carbon (DOC) concentrations follow the dominant scales of variation for both the control and slough wells but not for the landfill well. The wavelet power spectrum (Figure 13b) and global wavelet spectrum (Figure 13c) for the landfill (IC 36) well suggest that although the annual periodic component carries significant power (50% confidence interval), the dominant frequency may well lie outside the time scale of analysis. This is expected as the temporal variability in DOC concentrations are not limited to hydrologic events. Changes in the carbon content as a result of organic degradation can itself contribute to the temporal variability in the data [Cozzarelli *et al.*, 2011].

5. Conclusions and Discussion

[41] Biogeochemical processes and redox reactions are often characterized by high temporal variability. Analyses of biogeochemical data sets using correlation, principal component analysis, or other statistical techniques are not always able to identify the processes driving this temporal variability. Therefore, the focus of this study is to extract the complex linkages among biogeochemical processes and identify the temporal scales at which they exert dominant control using wavelet analysis.

[42] The wavelet analysis (CWT) reveals that the chemical data set of the Norman landfill site has single-scale characteristics (annual periodic component) for different geochemical variables at the landfill (IC 36) and control (IC South) wells despite the large differences in their geochemical characteristics and conceptual redox frameworks. Wavelet decomposition analysis further suggests that variations in concentrations of reactive and conservative solutes are strongly coupled to hydrologic variability at the dominant scale of variation. Moderate associations obtained using correlation analysis is suggestive of the fact that relationship between hydrologic data and geochemical concentration response is not linear but affected by coupled processes. Apart from hydrologic fluctuations (water table variations and precipitation events), temporal variability in sulfate concentrations can also be associated with different sources (FeS cycling and aquifer composition) and sinks (uptake by vegetation) depending on the well location and proximity to the leachate plume. At the slough well (IC 54), the continuous wavelet transform suggests an additional scale of variation (biannual periodic component) for diverse geochemical variables such as DOC, sulfate, and bromide. Both local slough interactions and vegetation dynamics are shown to be important factors affecting the temporal distribution of chemical constituents at this well. A limitation of this analysis is that these associations with hydrologic data are based on correlation analysis while geochemical and ecological (vegetation) linkages are based on reasoning and knowledge about the site. Wavelet

decomposition analysis provides further information on exceptions to these dominant scale(s) of variation. First, nitrate displays a multiscale behavior, which suggests that nitrate concentrations are influenced by several concomitant processes (such as plant decay, microbiological decomposition, and effect of climate). Second, the dominant variability in dissolved organic carbon concentrations is larger than 2 years at the landfill well. This behavior is not unexpected as several studies have documented the persistence of organic carbon at the Norman landfill site [Cozzarelli *et al.*, 2000, 2011; Eganhouse *et al.*, 2001]. Thus, wavelet analysis is able to reveal the complex variability of the biogeochemical data set at the Norman landfill site and extract specific frequencies that can be linked to the individual eco-hydrogeologic framework of the well location.

[43] Based on our analysis of the biogeochemical data set of 2 years, we hypothesize that the information in conservative and redox signals at annual time scales is guided by hydrologic events, while chemical concentrations at biannual time scales is governed by site-specific interactions (such as seasonality of vegetation and surface-groundwater dynamics). This can be corroborated by previous investigations that have demonstrated the effect of hydrogeological heterogeneities and seasonal influences on short-term variations in landfill leachate chemistry [Heron *et al.*, 1998; Kjeldsen *et al.*, 1998; Scholl *et al.*, 2006; Mangimbulude *et al.*, 2009]. At even larger time scales, these concentrations can be explained by linked biogeochemical processes such as increased xenophobicity of the carbon content (Figure 14). A 10 year study at the Vejen landfill linked the fate of certain xenobiotic compounds (benzene, herbicide Mecoprop) to the anaerobic conditions, and the recalcitrance of nonvolatile organic carbon to the depletion of iron reduction capacity within the aquifer [Baun *et al.*, 2003]. Similarly, 12 year data from the Dyer Boulevard Landfill suggested temporal trends in iron and manganese to be related to the reducing microbial environment of the site [Statom *et al.*, 2004]. Long-term studies at the Norman Landfill site also reported attenuation of ammonium by aquifer sediments and methane by oxidation in the center and upper boundary of the plume [Cozzarelli *et al.*, 2011]. In their review, Christensen *et al.* [2001] clearly indicated that several processes affecting landfill leachate, such as dilution, redox zonation, and microbial activity, are a function of both the local biogeochemistry and leachate composition. Figure 14 thus summarizes the temporal characteristics of redox-sensitive chemicals (barring extreme climatological events, natural disasters, and human intervention activities) at similar contaminated alluvial aquifers. This figure serves as a recommendation to evaluate linked biogeochemical factors in effectively accounting for long-term leachate trends and establishing regulatory controls.

[44] **Acknowledgment.** This project was supported by the National Science Foundation (grant EAR 0635961).

References

- Addison, P. S. (2005), Wavelet transforms and the ECG: A review, *Physiol. Meas.*, 26, 155–199.
- Asseng, S., I. R. P. Fillery, F. X. Dunin, B. A. Keating, and H. Meinke (2001), Potential deep drainage under wheat crops in a Mediterranean

- climate: I. Temporal and spatial variability, *Aust. J. Agric. Res.*, 52, 45–56.
- Báez-Cazull, S. E., J. T. McGuire, I. M. Cozzarelli, and M. A. Voytek (2008), Determination of dominant biogeochemical processes in a contaminated aquifer-wetland system using multivariate statistical analysis, *J. Environ. Qual.*, 37, 30–46, doi:10.2134/jeq2007.0169.
- Baun, A., L. Ask, A. Ledin, T. H. Christensen, and P. L. Bjerg (2003), Natural attenuation of xenobiotic organic compounds in a landfill leachate plume (Vejen, Denmark), *J. Contam. Hydrol.*, 65, 269–291.
- Becker, C. J. (2002), Hydrogeology and leachate plume delineation at a closed municipal landfill, Norman, Oklahoma, *U.S. Geol. Surv. Water Resour. Invest. Rep. 01–4168*, 36 pp.
- Beecham, S., and R. K. Chowdhury (2010), Temporal characteristics and variability of point rainfall: A statistical and wavelet analysis, *Int. J. Climatol.*, 30, 458–473.
- Bjerg, P. L., H. J. Albrechtsen, P. Kjeldsen, T. H. Christensen, and I. Cozzarelli (2003), The groundwater geochemistry of waste disposal facilities, in *Treatise on Geochemistry, Environmental Geochemistry*, vol. 9, edited by H. D. Holland, K. K. Turekian, and B. Sherwood Lollar, pp. 579–612, Elsevier, New York.
- Bjerg, P. L., N. Tuxen, L. A. Reitzel, H. J. Albrechtsen, and P. Kjeldsen (2011), Natural attenuation processes in landfill leachate plumes at three Danish sites, *Ground Water*, 49(5), 688–705.
- Bloschl, G., and M. Sivapalan (1995), Scale issues in hydrological modeling: A review, *Hydrol. Processes*, 9, 251–290.
- Breit, G. N., M. L. W. Tuttle, I. M. Cozzarelli, S. C. Christenson, J. B. Jaeschke, D. L. Fey, and C. J. Berry (2005), Results of chemical and isotopic analyses of sediment and ground water from alluvium of the Canadian river near a closed municipal landfill, Norman, Oklahoma, Part 2, *U.S. Geol. Surv. Open File Rep. 2008–1134*, 35 pp.
- Champ, D. R., J. Gulens, and R. E. Jackson (1979), Oxidation-reduction sequences in groundwater flow systems, *Can. J. Earth Sci.*, 127, 85–108.
- Chapelle, F. H. (2001), *Ground-Water Microbiology and Geochemistry*, John Wiley, New York.
- Christensen, T. H., P. L. Bjerg, S. Banwart, R. Jakobsen, G. Heron, and H.-J. Albrechtsen (2000), Characterization of redox conditions in groundwater contaminant plumes, *J. Contam. Hydrol.*, 45(3–4), 165–241.
- Christensen, T. H., P. Kjeldsen, P. L. Bjerg, D. L. Jensen, J. B. Christensen, A. Baun, H.-J. Albrechtsen, and G. Heron (2001), Biogeochemistry of landfill leachate plumes, *Appl. Geochem.*, 16, 659–718.
- Christenson, S., M. A. Scholl, J. L. Schlottmann, and C. J. Becker (1999), Ground-water and surface-water hydrology of the Norman Landfill Research Site, in *Toxic Substances Hydrology Program—Proceedings of the Technical Meeting*, *U.S. Geol. Surv. Water Resour. Invest. Rep. 99–4018C*, pp. 501–507.
- Comrie, A. C., and E. C. Glenn (1998), Principal components-based regionalization of precipitation regimes across the southwest United States and northern Mexico, with an application to monsoon precipitation variability, *Clim. Res.*, 10, 201–215.
- Cozzarelli, I. M., J. M. Sufita, G. A. Ulrich, S. H. Harris, J. L. Schlottmann, and S. Christenson (2000), Geochemical and microbiological methods for evaluating anaerobic processes in an aquifer contaminated by landfill leachate, *Environ. Sci. Technol.*, 34(18), 4025–4033.
- Cozzarelli, I. M., B. A. Bekins, M. J. Baedeker, G. R. Aiken, R. P. Eganhouse, and M. E. Tuccillo (2001), Progression of natural attenuation processes at a crude-oil spill site: I. Geochemical evolution of the plume, *J. Contam. Hydrol.*, 53(3–4), 369–385.
- Cozzarelli, I. M., J. K. Bohlke, J. Masoner, G. N. Breit, M. M. Lorah, M. L. W. Tuttle, and J. B. Jaeschke (2011), Biogeochemical evolution of a landfill leachate plume, Norman, Oklahoma, *Ground Water*, 49(5), 663–687.
- Das, N. N., and B. P. Mohanty (2008), Temporal dynamics of PSR-based soil moisture across spatial scales in an agricultural landscape using SMEX02: A wavelet approach, *Remote Sens. Environ.*, 112, 522–534.
- Daubechies, I. (1992), *Ten Lectures on Wavelets*, SIAM, Philadelphia, Pa.
- Diou, A., C. Dumont, O. Lalignant, M. Toubin, F. Truchetet, E. P. Verrecchia, M. A. Abidi (1999), Multiscale analysis of range image: Its use for growth increment characterization, *Opt. Eng.*, 38(12), 2016–2021.
- Eganhouse, R. P., I. M. Cozzarelli, M. A. Scholl, and L. L. Matthews (2001), Natural attenuation of volatile organic compounds (VOCs) in the leachate plume of a municipal landfill: Using alkylbenzenes as a process probe, *Ground Water*, 39(2), 192–202.
- Farge, M. (1992), Wavelet transforms and their applications to turbulence, *Annu. Rev. Fluid Mech.*, 24, 395–457.
- Fendorf, S., H. A. Michael, and A. van Geen (2010), Spatial and temporal variations of groundwater arsenic in south and Southeast Asia, *Science*, 328(5982), 1123–1127.
- Foufoula-Georgiou, E., and P. Kumar (1994), *Wavelets in Geophysics*, Academic, San Diego, Calif.
- Fugal, D. L. (2009), *Conceptual Wavelets in Digital Signal Processing*, Space and Signals Tech. Publ., San Diego, Calif.
- Geesey, G. G., and A. C. Mitchell (2008), Need for direct measurements of coupled microbiological and hydrological processes at different scales in porous media systems, *J. Hydrol. Eng.*, 13, 28–36.
- Grinsted, A., S. Jevrejeva, and J. Moore (2004), Application of the cross-wavelet transform and wavelet coherence to geophysical time series, *Non-linear Processes Geophys.*, 11, 561–566.
- Grossman, E. L., L. A. Cifuentes, and I. M. Cozzarelli (2002), Anaerobic methane oxidation in a landfill-leachate plume, *Environ. Sci. Technol.*, 36(11), 2436–2442.
- Guan, K., S. E. Thompson, C. J. Harman, N. B. Basu, P. S. C. Rao, M. Sivapalan, A. I. Packman, and P. K. Kalita (2011), Spatiotemporal scaling of hydrological and agrochemical export dynamics in a tile-drained Midwestern watershed, *Water Resour. Res.*, 47, W00J02, doi:10.1029/2010WR009997.
- Haack, S. K., and B. A. Bekins (2000), Microbial populations in contaminant plumes, *Hydrogeol. J.*, 8(1), 63–76.
- Haack, S. K., L. R. Fogarty, T. G. West, E. W. Alm, J. T. McGuire, D. T. Long, D. W. Hyndman, and L. J. Forney (2004), Spatial and temporal changes in microbial community structure associated with recharge-influenced chemical gradients in a contaminated aquifer, *Environ. Microbiol.*, 6(5), 438–448.
- Hariprasath, S., and V. Mohan (2009), Iris pattern recognition using complex wavelet and wavelet packet transform, *J. Comput. Appl.*, 2(2), 18–23.
- Harris, S. H. Jr, J. D. Istok, and J. M. Sufita (2006), Changes in organic matter biodegradability influencing sulfate reduction in an aquifer contaminated by landfill leachate, *Microb. Ecol.*, 51(4), 535–542.
- Heron, G., and T. H. Christensen (1995), Impact of sediment bound iron on redox buffering in a landfill polluted aquifer (Vejen, Denmark), *Environ. Sci. Technol.*, 29, 187–192.
- Heron, G., P. L. Bjerg, P. Gravesen, L. Ludvigsen, and T. H. Christensen (1998), Geology and sediment geochemistry of a landfill leachate contaminated aquifer (Grindsted, Denmark), *J. Contam. Hydrol.*, 29(4), 301–317.
- Hunter, K. S., Y. Wang, and P. van Cappellen (1998), Kinetic modeling of microbially-driven redox chemistry of subsurface environments: Coupling transport, microbial metabolism, and geochemistry, *J. Hydrol.*, 209, 53–80.
- Jana, R. B., and B. P. Mohanty (2012), On topographic controls of soil hydraulic parameter scaling at hill-slope scales, *Water Resour. Res.*, 48, W02518, doi:10.1029/2011WR011204.
- Jardine, P. M. (2008), Influence of coupled processes on contaminant fate and transport in subsurface environments, *Adv. Agron.*, 99, 1–99, doi:10.1016/S0065–2113(08)00401-X.
- Jolley, D. M., T. F. Ehrhorn, and J. Horn (2003), Microbial impacts to the near-field environment geochemistry: A model for estimating microbial communities in repository drifts at Yucca Mountain, *J. Contam. Hydrol.*, 62–63, 553–575.
- Kamolpornwijit, W., L. Liang, O. R. West, G. R. Moline, A. B. Sullivan (2003), Preferential flow path development and its influence on long-term PRB performance: Column study, *J. Contam. Hydrol.*, 66(3–4), 161–178.
- Kia, S. H., H. Henao, and G.-A. Capolino (2009), Diagnosis of broken-bar fault in induction machines using discrete wavelet transform without slip estimation, *IEEE Trans. Ind. Appl.*, 45(4), 1395–1404.
- Kjeldsen, P., P. L. Bjerg, J. K. Pedersen, K. Rügge, and T. H. Christensen (1998), Characterization of an old municipal landfill (Grindsted, Denmark) as a groundwater pollution source: Landfill hydrology and leachate migration, *Waste Manage. Res.*, 16(1), 14–22.
- Kumar, P., and E. Foufoula-Georgiou (1997), Wavelet analysis for geophysical applications, *Rev. Geophys.*, 35(4), 385–412.
- Kusel, K. (2003), Microbial cycling of iron and sulfur in acidic coal mining lake sediments, *Water Air Soil Pollut.*, 3(1), 67–90.
- Labat, D., R. Ababou, and A. Mangin (2000), Rainfall-runoff relations for karstic springs. Part II: Continuous wavelet and discrete orthogonal multiresolution analyses, *J. Hydrol.*, 238, 149–178.
- Langmuir, D. (1997), *Aqueous Environmental Geochemistry*, Prentice Hall, Upper Saddle River, N. J.

- Lau, K.-M., and H. Weng (1995), Climate signal detection using wavelet transform: How to make a time series sing, *Bull. Am. Meteorol. Soc.*, 76(12), 2391–2402.
- Lorah, M. M., I. M. Cozzarelli, and J. K. Böhlke (2009), Biogeochemistry at a wetland sediment-alluvial aquifer interface in a landfill leachate plume, *J. Contam. Hydrol.*, 105(3–4), 99–117.
- Lovley, D. R., and F. H. Chapelle (1995), Deep subsurface microbial processes, *Rev. Geophys.*, 33, 365–381.
- Mallat, S. (1999), *A Wavelet Tour of Signal Processing*, Academic, New York.
- Mangimbulude, J. C., B. M. van Breukelen, A. S. Krave, N. M. van Straalen, and W. F. M. Röling (2009), Seasonal dynamics in leachate hydrochemistry and natural attenuation in surface run-off water from a tropical landfill, *Waste Manage.*, 29(2), 829–838.
- Maraun, D., and J. Kurths (2004), Cross-wavelet analysis: Significance testing and pitfalls, *Nonlinear Processes Geophys.*, 11, 505–514.
- Martinez, B., and M. A. Gilabert (2009), Vegetation dynamics from NDVI time series analysis using the wavelet transform, *Remote Sens. Environ.*, 113, 1823–1842.
- McGuire, J. T., E. W. Smith, D. T. Long, D. W. Hyndman, S. K. Haack, M. J. Klug, and M. A. Velbel (2000), Temporal variations in parameters reflecting terminal-electron-accepting processes in an aquifer contaminated with waste fuel and chlorinated solvents, *Chem. Geol.*, 169(3–4), 471–485.
- McGuire, J. T., D. T. Long, M. J. Klug, S. K. Haack, and D. W. Hyndman (2002), Evaluating behavior of oxygen, nitrate, and sulfate during recharge and quantifying reaction rates in a contaminated aquifer, *Environ. Sci. Technol.*, 36(12), 2693–2700.
- Megonigal, J. P., M. E. Hines, and P. T. Visscher (2004), *Anaerobic Metabolism: Linkages to Trace Gases and Anaerobic Processes*, Elsevier, Oxford, U. K.
- Mercer, J. W. (1983), *The Role of the Unsaturated Zone in Radioactive and Hazardous Waste Disposal*, Butterworth-Heinemann, Oxford, U. K.
- Merry, R., and M. Steinbuch (2005), Wavelet theory and applications: A literature study, Dep. of Mech. Eng., Control Syst. Technol. Group, Eindhoven Univ. of Technol., Eindhoven, Netherlands.
- Mills, A. L., P. E. Bell, and A. T. Herlihy (1989), Microbes, sediments, and acidified waters: The importance of biological buffering, in *Acid Stress and Aquatic Microbial Interactions*, edited by S. S. Rao, pp. 1–19, CRC Press, Boca Raton, Fla.
- Milne, A. E., C. J. A. Macleod, P. M. Haygarth, J. M. B. Hawkins, and R. M. Lark (2009), The wavelet packet transform: A technique for investigating temporal variation of river water solutes, *J. Hydrol.*, 379, 1–19.
- Misiti, M., Y. Misiti, G. Oppenheim, and J. M. Poggi (2008), *MATLAB User's Guide: Wavelet Toolbox™ 4*, The Math Works Inc, Natick, Mass.
- Mitchell, C. P. J., and B. A. Branfireun (2005), Hydrogeomorphic controls on reduction–oxidation conditions across boreal upland–peatland interfaces, *Ecosystems*, 8(7), 731–747.
- Mukherjee, A., M. von Brömssen, B. R. Scanlon, P. Bhattacharya, A. E. Fryar, M. A. Hasan, K. M. Ahmed, D. Chatterjee, G. Jacks, and O. Sraček (2008), Hydrogeochemical comparison and effects of overlapping redox zones on groundwater arsenic near the Western (Bhagirathi sub-basin, India) and Eastern (Meghna sub-basin, Bangladesh) margins of the Bengal Basin, *J. Contam. Hydrol.*, 99(1–4), 31–48.
- Pacific, V. J., B. L. McGlynn, D. A. Riveros-Iregui, D. L. Welsch, and H. E. Epstein (2011), Landscape structure, groundwater dynamics, and soil water content influence soil respiration across riparian-hillslope transitions in the Tenderfoot Creek Experimental Forest, *Montana, Hydrol. Processes*, 25(5), 811–827.
- Partal, T. (2012), Wavelet analysis and multi-scale characteristics of the runoff and precipitation series of the Aegean region (Turkey), *Int. J. Climatol.*, 32(1), 108–120.
- Percival, D. B. (2008), Analysis of geophysical time series using discrete wavelet transforms: An overview, in *Lecture Notes in Earth Sciences*, vol. 112, edited by R. V. Donner and S. M. Barbosa, pp. 61–79, Springer, Berlin.
- Percival, D. B., and A. T. Walden (2000), *Wavelet Methods for Time Series Analysis*, Cambridge Univ. Press, Cambridge, U. K.
- Qian, J., and K. Mopper (1996), Automated high performance, high temperature combustion total organic carbon analyzer, *Anal. Chem.*, 68, 3090–3097.
- Quiroz, R., C. Yarleque, A. Posadas, V. Mares, and W. W. Immerzeel (2011), Improving daily rainfall estimation from NDVI using a wavelet transform, *Environ. Modell. Software*, 26, 201–209.
- Raz-Yaseef, N., E. Rotenberg, and D. Yakir (2010), Effects of spatial variations in soil evaporation caused by tree shading on water flux partitioning in a semi-arid pine forest, *Agric. Forest Meteorol.*, 150, 454–462.
- Röling, W. F. M., B. M. van Breukelen, M. Braster, B. Lin, and H. W. van Verseveld (2001), Relationships between microbial community structure and hydrochemistry in a landfill leachate-polluted aquifer, *Appl. Environ. Microbiol.*, 67(10), 4619–4629.
- Sang, Y.-F. (2012), A practical guide to discrete wavelet decomposition of hydrologic time series, *Water Resour. Manage.*, 26, 3345–3365.
- Schlottmann, J. L. (2001), Water chemistry near the closed Norman Landfill, Cleveland County, Oklahoma, 1995, *U.S. Geol. Surv. Water Resour. Invest. Rep. 00–4238*, 44 pp.
- Scholl, M. A., and S. C. Christenson (1998), Spatial variation in hydraulic conductivity determined by slug tests in the Canadian River alluvium near the Norman Landfill, Norman, Oklahoma, *U.S. Geol. Surv. Water Resour. Invest. Rep. 97–4292*, 28 pp.
- Scholl, M. A., S. C. Christenson, and I. M. Cozzarelli (2005), Recharge processes in an alluvial aquifer riparian zone, Norman Landfill, Norman, Oklahoma, 1998–2000, *U.S. Geol. Surv. Water Resour. Invest. Rep. 2004–5238*, 60 pp.
- Scholl, M. A., I. M. Cozzarelli, and S. C. Christenson (2006), Recharge processes drive sulfate reduction in an alluvial aquifer contaminated with landfill leachate, *J. Contam. Hydrol.*, 104(3–4), 4–35.
- Shao, X.-G., A. K.-M. Leung, and F.-T. Chau (2003), Wavelet: A new trend in chemistry, *Acc. Chem. Res.*, 36(4), 276–283.
- Sinke, A. J. C., O. Dury, and J. Zobrist (1998), Effects of a fluctuating water table: Column study on redox dynamics and fate of some organic pollutants, *J. Contam. Hydrol.*, 33(1–2), 231–246.
- Smith, K. S. (2007), Strategies to predict metal mobility in surficial mining environments, in *Reviews in Engineering Geology, Volume XVII: Understanding and Responding to Hazardous Substances at Mine Sites in the Western United States*, edited by J. V. DeGraff, pp. 25–45, The Geol. Soc. of Am., Boulder, Colo.
- Statom, R. A., G. D. Thyne, and J. E. McCray (2004), Temporal changes in leachate chemistry of a municipal solid waste landfill cell in Florida, USA, *Environ. Geol.*, 45(7), 982–991.
- Taylor, S. W., and P. R. Jaffe (1990), Biofilm growth and the related changes in the physical properties porous medium, *Water Resour. Res.*, 26(9), 2153–2159.
- Torrence, C., and G. P. Compo (1998), A practical guide to wavelet analysis, *Bull. Am. Meteorol. Soc.*, 79(1), 61–78.
- Tuttle, M. L. W., G. N. Breit, and I. M. Cozzarelli (2009), Processes affecting $\delta^{34}\text{S}$ and $\delta^{18}\text{O}$ values of dissolved sulfate in alluvium along the Canadian River, central Oklahoma, USA, *Chem. Geol.*, 265, 455–467.
- Tuxen, N., H.-J. Albrechtsen, and P. L. Bjerg (2006), Identification of a reactive degradation zone at a landfill leachate plume fringe using high resolution sampling and incubation techniques, *J. Contam. Hydrol.*, 85(3–4), 179–194.
- Ulrich, G. A., G. N. Breit, I. M. Cozzarelli, and J. M. Suffita (2003), Sources of sulfate supporting anaerobic metabolism in a contaminated aquifer, *Environ. Sci. Technol.*, 37(6), 1093–1099.
- Van Breukelen, B. M., W. F. M. Röling, J. Groen, J. Griffioen, and H. W. Van Verseveld (2003), Biogeochemistry and isotope geochemistry of a landfill leachate plume, *J. Contam. Hydrol.*, 65(3–4), 245–268.
- Wanty, R. B., and B. R. Berger (2006), Geologic, hydrologic, and geochemical interpretations of mineral deposits as analogs for understanding transport of environmental contaminants, *J. Geochem. Explor.*, 88, 162–165.
- Zhang, Q., C. Liu, C.-Y. Xu, Y. Xu, and T. Jiang (2006), Observed trends of annual maximum water level and streamflow during past 130 years in the Yangtze River basin, China, *J. Hydrol.*, 324(1–4), 255–265.